

ACTIVE AND PASSIVE
COASTAL PAVEMENT
DEGRADATION

URBAN DOCUMENTATION CENTRE
RESEARCH UNIT FOR URBAN STUDIES
McMASTER UNIVERSITY
HAMILTON, ONTARIO

By

JAMES ANDREW HYATT

A Research Paper

Submitted to the Department of Geography

in Fulfilment of the Requirements

of Geography 4C6

McMaster University

April 1985

007476

ABSTRACT

Inland degradational trends of coastal dolomite pavements (on the Amabel formation near Tobermory Ontario - Map 1) were examined in three wave energy settings: passive, intermediate, and active shores.

Six pavement property trends were examined to determine the effect of low fetch lengths (7-10 km - Ford 83) and long shallow wave approach (Map 1) on the break-up of passive coastal pavements (south-west Bear's Rump Island): vegetation cover, grike dimensions, fracturing, pitting, shattering and flaking, and soil and rubble depths.

Detailed analysis of small scale surface solution features, "karren", was undertaken at five 1 m sample grids on the intermediate average fetch 70-90 km - Grosset 85) Cyprus Lake provincial park pavements.

Pavement disintegration on the active northeast coast of Bear's Rump Island (average fetch of 75 - 100 km - Ford 83 - and a steep bathimetric profile) was indexed by dimensional changes in solution corroded joints or "grikes".

Master bedding surfaces, present and past lake levels, and vegetation were found to be the dominant controls on inland pavement disintegration for active and passive coasts. The first two factors were more important to pavement break-up on south-west passive Bear's Rump, while the latter gained potency on the wave attacked north-east shore. The effect of vegetation intensified solution on grike width, a pavement condition index, was quantified (Appendix III) and expressed in terms of maximum added width (in meters) at given inland distances.

Four surface trends, dependent on distance from water, exist on Cyprus Lake pavements; karren variety, surface morphology, exposure age, and vegetation cover. Vegetation effect on grike width (Appendix III) was calculated in the same manner as the active Bear's Rump examples.

ACKNOWLEDGEMENTS

I would like to express my gratitude to Dr. Derek Ford for the guidance and funding necessary to complete this paper. Also, Dr. John Drake for his helpful suggestions regarding statistical analysis.

Thanks as well to Steve Worthington and Nigel Roulet for assistance with the computer, and Patrick Folke for accomodation and water transportation while in Tobermory.

TABLE OF CONTENTS

ABSTRACT	ii
ACKNOWLEDGEMENT	iii
TABLE OF CONTENTS	iv
LIST OF FIGURES	vi
LIST OF TABLES	viii
Chapter	
1.0 INTRODUCTION TO THE STUDY AREA	1
1.1 Relevant Definitions	1
1.2 Study Hypothesis	1
1.3 Local Geology	2
1.4 Pavement Modification	6
1.5 Coastal karst	9
1.6 Data Acquisition	11
2.0 PASSIVE SHORELINE PAVEMENT DEGRADATION	13
2.1 Vegetation Cover and Grike Condition trends	13
Conclusions	16
2.2 Pitting Trends	17
Conclusions	20
2.3 Fracture - Flaking and Shatter Trends	21
Conclusions	24
2.4 Soil and Rubble Depth Trends	24
Conclusions	26
3.0 INTERMEDIATE SHORELINE PAVEMENT DEGRADATION	27
3.1 Detailed Karren Analysis - Cyprus Lake	27
3.2 Hand Specimen Analysis	31
3.3 Conclusions	32
4.0 ACTIVE SHORELINE PAVEMENT DEGRADATION	33
4.1 Dependent Variables: Grike Width and Depth	33
4.2 Independent Variables	34
4.2.(i) Wave Attack	34
4.2.(ii) Grike Fill	35
4.2.(iii) Bedrock Properties	39
Conclusions	41

5.0	SUMMARY OF CONCLUSIONS	42
APPENDIX I	Chemistry of Carbonate Rock Dissolution	44
APPENDIX II	Grike Measurement Station Location	7
	a) Graphical Method	
	b) Numerical Method	
APPENDIX III	A/ Statistical Comparison of Grike Dimension	54
	Change Between Sample Sites	
	B/ Vegetation Effect Determination	59
APPENDIX IV	Grike Dimension Vs. Distance to Water	61
APPENDIX V	Determining Insoluble Percentage	65
APPENDIX VI	Plates From Text	67
APPENDIX VII	Inland Pavement Example	75
	LIST OF ABBREVIATIONS	80
	BIBLIOGRAPHY	81

LIST OF FIGURES

Figure		Page
Map 1.0	Study Area	16
1.5.1	Coastal zones of BRI (Ford 85)	10
2.1.1 a)	Multiple, Single and Micro Pits	18
2.2.2	Pit Shelf Location	18
2.2.3	Master Bedding Surface Control	20
2.2.4	Georgian Bay Lake Levels	20
2.2.5	Stepwise Degradation Pattern	20
2.2.6	Freeze Thaw Location	21
2.3.1	Passive Shore Station Morphology	22
2.4.1	Inverse Relation-between soil and rubble depth	25
2.4.2	Lag-of rank of soil and rubble depth	25
3.2.1	Hand Specimen End Members	32
4.1.1	Grike Measurement Problems	33
4.2.1	Plan View and Cross-Section of BRI SS#1	34
4.2.2	Data Refinement Example	35
4.2.4 a-f	Data Refinement Procedure	36b
4.2.5	Hydraulic Head, MBS, Control on Grike width	38
AI.1	Co ₂ Dissolution in Atmosphere	44
AII.1a	Plan View of Sample Strip #2 BRI	47
AII.1b	Cross-section of SS#2 BRI	47
AII.2a,b	Plan and Cross-section SS#1 BRI	49
AII.3a,b	Plan and Cross-section SS#2 BRI	50
AII.4a,b	Plan and Cross-section SS#3 BRI	51
AII.5	Plan view Cyprus Lake SS#1	51
AII.6a,b	Plan and Cross-section Cyprus Lake SS#2	53
AIII.1	Dimensional Limits of SS#1 BRI width and depth vs Distance to Water	54
AIV.1	Summary Diagram Grike width vs distance to shore BRI SS #1	61
AIV.2	Summary Diagram Grike width vs distance to shore BRI SS #2	61
AIV.3	Summary Diagram Grike width vs distance to shore BRI SS #3	62
AIV.4	Summary Diagram Grike width vs distance to shore CYPRUS LAKE SS #1	62
AIV.5	Summary Diagram Grike width vs distance to shore CYPRUS LAKE SS #2	63
AIV.6	Summary Diagram Grike depth vs distance to shore BRI SS #1	63
AIV.7	Summary Diagram Grike depth vs distance to shore BRI SS #2	64
AIV.8	Summary Diagram Grike depth vs distance to shore BRI SS #3	64
AV.1	Moisture Equilibrium - sample weight	66

AV.2	Moisture Equilibrium - Filter paperweight	67
Plate AVI.1	Coarse Break up, Shattered Rock	68
Plate AVI.2	Shattered stationary fracture	69
Plate AVI.3	Flaked Rock Fragments	70
Plate AVI.4	Detailed Karren site K1 Cyprus Lake	72
Plate AVI.5	Detailed Karren site K2 Cyprus Lake	72
Plate AVI.6	Detailed Karren site K3 Cyprus Lake	73
Plate AVI.7	Detailed Karren site K4 Cyprus Lake	74
Plate AVI.8	Detailed Karren site K5 Cyprus Lake	74
AVIII.1	Plan View of Dyer's Bay Sample Site	76
Plate AVII.1	Roadside View of Dyer's Bay Sample Site	77
Plate AVII.2	Centre Piece in Grike G3	78
Plate AVII.3	Pit Bottom of Rundkarren channel	79

LIST OF TABLES

1.2.1	Independent and Dependent Variables of Analysis	4
2.0.1	Passive Pavement Property Ranks	13
2.1.1	Vegetation Summary L1-6 to L1-10	16
AIII.1a	Grike Width's Statistical Analysis	58
AIII.1b	Grike Depth Statistical Analysis	59
AIII.2	Vegetation Effect Equations	60
AV.1	Insoluble Percentage Calculation	66
AVI.1	Karren Analysis Characteristics - Cyprus Lake	70

1.0 CHAPTER INTRODUCTION

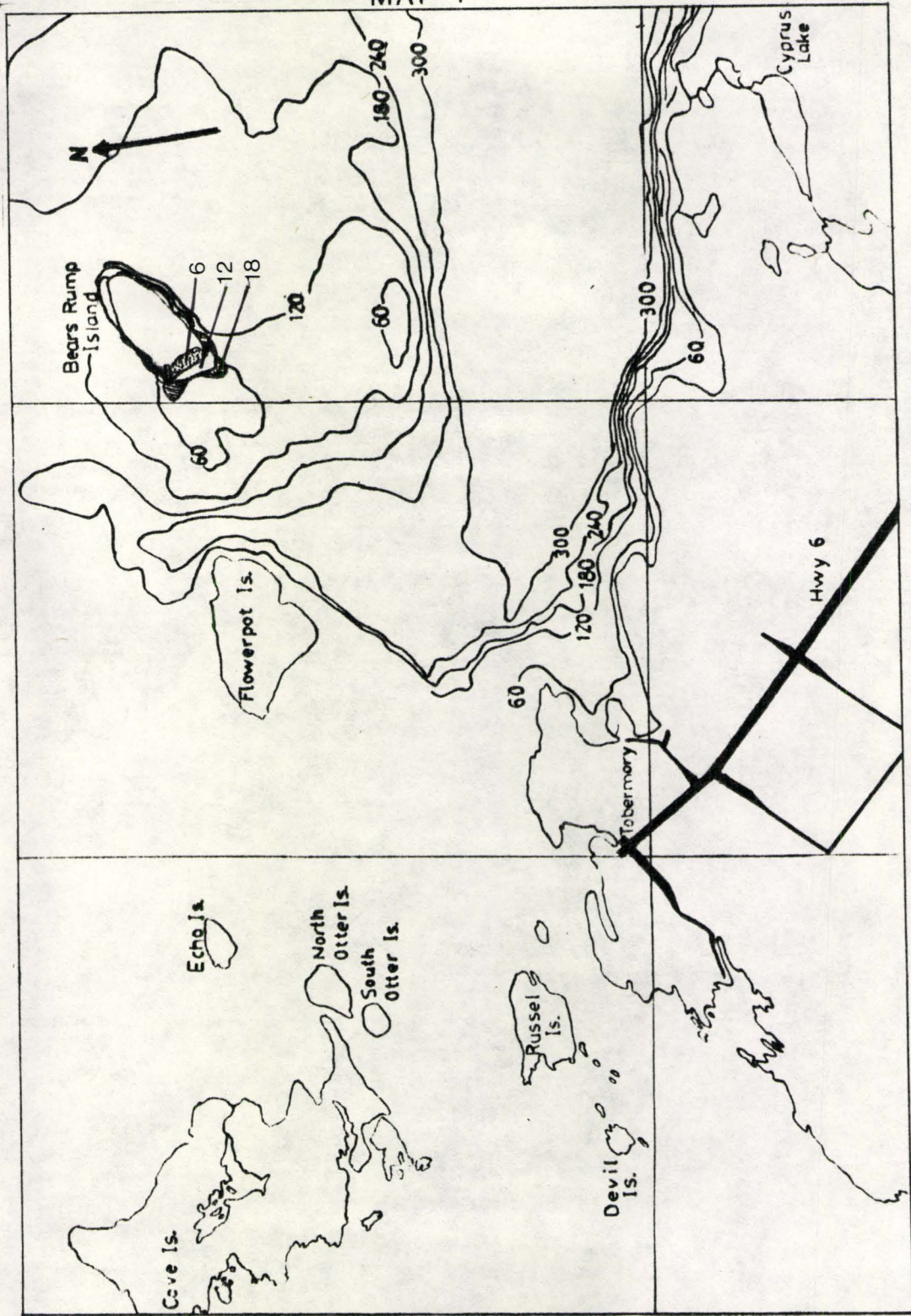
The purpose of this thesis is to analyse the nature of coastal dolomite pavement and its degradation inland on active, intermediate and passive shorelines. Data was collected chiefly from Bear's Rump Island located in Georgian Bay just off of Tobermory (Map 1.0). There were two additional mainland sample sites at Cyprus Lake Provincial Park and Dyers Bay. This introduction will define terms, describe local geology and modifications, describe coastal karsts, and outline the sampling method employed in the field.

1.1 RELEVANT DEFINITIONS

Karst - The main geomorphic process at work in the study area is the dissolution and selective removal of dolomite bedrock. This is known as "Karstification" and its effects are observed on the Bruce Peninsula outcrops examined. There are generally three classifications of Karst namely holokarst (perfectly developed karst landforms with a subterranean hydrologic system), merokarst (imperfect karst generally soil covered with minor underground development), and transitional karst (between end members showing deep Karstic forms) [Sweeting 72, Cvijic]. Another class suggested by Jennings is free karst; which is karst that can drain directly into the sea without intervention of different hydrological systems [Jennings 71]. This is the Karst class of Bear's Rump Island where there is simple surface and ground water drainage to the lake.

Karren - The result of karst processes on the dolomites are distinctive small scale surface corrosional patterns known as "karren". Five varieties of karren; kluft karren, pit karren, rund karren, spitz

MAP 1



karren and Kamenitzas, were observed in the field area. Solutional exploitation, usually along master joint systems (largest, most regular but widely spaced joints) [Ford 85 - thesis suggestion] lead to widened fissures known as "Kluft Karren" or grikes. These fissures slice the surface into a series of blocks or clints thus the term "clint and grike topography."

Karst Pavement - Any process which scours and strips off layers of bedrock can produce a flat surface, "pavement", upon which solutional indentation such as Kluft Karren may occur [Ford 85]. Such morphologies are common on carbonate rock, the glacially scoured Amabel dolomites of the Bruce Peninsula are no exception.

Active & Passive Shorelines - A high energy coast occurs where there is considerable fetch (obstruction-free water over which waves build) and relatively deep water close to shore which allows waves to expend energy directly on the shore. The NW side of Bear's Rump Island is the studied example of such an "active" coast. In contrast "passive" coasts have shorter fetches and a shallow shelf extending offshore, causing waves to break before they reach land. An example is the south shore of Bear's Rump Island. The Cyprus Lake Provincial Park shoreline is intermediate between the two end members.

1.2 STUDY HYPOTHESES

Pavement degradation is a rather vague phrase. It is in need of indexing to permit qualitative and quantitative analysis. This may be accomplished by examining changes in individual properties of the pavement.

Grike dimensions are one of the properties considered. Pavement fades to obscurity inland (on BRI) and grike widths and depths also become less clear away from the water. Since the grikes and pavement (as a whole) appear to degrade in a similar fashion grike dimensions may be indicative of the degradational state of the pavement. The more pronounced development of grikes near the shoreline could be due to increased hydraulic head (water draining to lake level over a shorter distance) [Ford 85], availability of fresh undersaturated lake water (for renewed dissolution), and removal of the saturated boundary layer by wave action (exposing fresh carbonate).

The grike dimension index of pavement condition is more powerful along active shorelines. This is because of fewer extraneous variables such as extensive vegetation fill, and clint fracturing or flaking. Therefore the first research hypothesis will deal with grike widths and depths on the active NW shore of BRI with the assumption that those dimensions are indicative of the overall pavement condition. It follows that independent variables influencing grike measurement also influence degradation. Therefore those independent variables are important to the understanding of pavement disintegration away from active coasts. The formal hypothesis is as follows:

HYPOTHESIS #1

Inland depth and width changes of grikes are due to

1. wave attack
2. bedrock properties
3. Grike fill

(Chapter 4)

Table 1.2.1 presents this hypothesis in the form of independent and dependent variable analysis.

Table #1.2.1

DEPENDENT VARIABLE	INDEPENDENT VARIABLES		
1.Grike Dimensions	1.Wave Attack	2.Bedrock Properties	3.Grike Fill
A,width	A.horizontal distance	A.joint orientation	A.vegetation
B.depth	B.vertical dist to water	B.grain size	B.rubble
		C.insoluble content	C.soil-dirt

The second hypothesis of this study (Chapter 2) deals with pavement changes on passive shorelines, Grike

dimensions alone are insufficient to describe the state of disintegration. Vegetation fill become more pronounced landward in the more habitable subaerial environment above normal wave attack. Other variables such as pitting, fracturing, and flaking also influence pavement break up. The interactions of those variables leads to a pattern of inland degradation which is the jist of the second hypothesis.

HYPOTHESIS #2

Passive pavement degradation involves a definite progressive change in

- a) vegetation cover
- b) rock fracturing - insitu-moved
- c) pitting
- d) shattering and flaking
- e) grike dimensions
- f) soil , rubble depth

A more descriptive approach to analysis will be employed.

Surface karren, an important descriptive aspect of karst pavements,

are affected by a degrading pavement. Consequently an analysis of pavement break-up would be incomplete unless detailed inland karren changes or trends were examined. Cyprus Lake afforded the greatest variety of karren; pits, grikes, kamenitzas, and rund karren and consequently used for detailed karren analysis (Chapter 3).

1.3 LOCAL GEOLOGY

Sampling for this thesis came from the Amabel Dolomite at the top of the Bruce Peninsula. The Amabel formation is stratigraphically situated between the Guelph Fm above and the Fossil Hill Fm below. The Amabel is comprised of 3 members; the Lions Head member - blocky, dense, weathered dark brown, the Colpoy Bay - Wiarton member - pure, locally thin bedded interreefal strata resistant to mechanical erosion, and the Ermosa member - thinly bedded interreefal deposits. Only the Wiarton member develops good solutional weathering features with a chemical composition of $\text{Ca}_{1.2}\text{Mg}_{0.8}\text{CO}_3$ [Cowell 76].

The Amabel and other formations of the upper Bruce Peninsula are located on the western rim of the Michigan basin, a depression of Cambrian age. Older shield rocks were weathered and transported into the basin causing slow subsidence. The Silurian climate was warm and created extensive shallow reefs with a general NE-SW orientation. Subsequent partial basin cut off increase salinities assisting in dolomitization of the carbonate reefs. The result is the resistant strata that is seen today. Some of these reefal structures are found in the Silurian aged Amabel formation found on the lower half of Bear's Rump Island and at Cyprus Lake

Provincial Park. Reefal bioherms and interreefal material of varying relative proportions and strengths form the flat, gently SW dipping (poorly developed) beds of the Amabel. Structuarally strong bioherms are usually situated between weaker, conforming interreefal beds which display intense construction joints (oriented 260-70/80-90, 320-30/140-50 on Bear's Rump Island) [Goodchild 84].

Much of the Amabel has been scoured by glaciers to form pavements some of which were studied for this report.

L.4 PAVEMENT MODIFICATION - Glaciation, Karren

Limestone (or dolomite) pavements result from scouring of limestone (dolomite) surfaces followed by solution [Sweeting 72, Jenning71, Chambers, many others]. In Canada glaciers have been the dominant scouring agent. Williams defines pavements as "roughly horizontal exposures of limestone (dolomite) bedrock, the surface of which is a) approximately parallel to bedding b) developed into a geometrical pattern of blocks formed by the intersections of widened fissures."

Goodchild provides a brief account of glacial effects on the local bedrock. The most recent glacial advance was impeded by the Niagara Escarpment and Algonquin Arch. These barriers prompted ice to move parallel to the peninsula. Intense glacial erosion occurred west of Cabot Head where the ice was forced to climb the escarpment. Only very resistant areas survived this erosion. Bear's Rump Island is one such area.

There are three types of factors affecting karren development. First, passive factors which involve relatively constant pavement properties such as petrology, porosity, bedding and jointing. Active features are

temperature, acidity of rain and soil water, and plant growth. Lastly there are historical factors, that is changes of controls over time (Jenning 71). The following is a list of specific factors which strongly influence pavement morphology.

- 1) Lithology [Jenning 71, Cowell 76, Pluhar 66, Sweeting 72]
- 2) Vegetation [Jenning 71, Cowell 76, Sweeting 72]
- 3) Climate - present and past [Jenning 71, Sweeting 72, Cowell 76]
- 4) Geologic structure [Jenning 71, Cowell 76, Pluhar 66, Sweeting 72]

Lithology is an encompassing term. It covers a wide range of properties characterized by bed properties, chemical and mineral properties, and porosity and permeability. Bed properties include bed thickness [Jenning 71]; closely spaced beds are detrimental to karren development due to insoluble material concentrating along the bedding planes [Ritter 78]. Texture [Sweeting 72]; fine grained carbonates restrict water penetration and therefore karren development to upper layers [Pluhar 66]. Chemical properties such as Silica concentration were investigated by Pluhar. She concluded that impurities, especially Si concentrations, hinder karren development due to interference in the solution process.

The main effect of vegetation is accelerated karstification [Sweeting 72]. Vegetation in the Bruce Peninsula occurs directly on exposed carbonate rocks or with a meter or so of overburden [Cowell 76] which acts as an acidic sponge [Jennings 71]. Partial vegetation due to incomplete soil removal or creation often generates solution pans (kamenitzas) [Jenning 71]. Total vegetation cover is effective in grike

expansion and rundkarren development. Direct lichen and moss growth on pavement can initiate small hollows [Watham, Cowell 76].

Weaker pavement rocks are more susceptible to frost action and flaking, consequently they are frequently grass covered [Waltham]. Vegetation thus aids in the solution of small surface karren. It is also possible that some of these karren can preserve ancient soils. Such is commonly the case with soil filled grikes [D. P. Drew 83].

Bedrock structure is very important to karren development. In the Tobermory area joints are the most influential structural feature. Joints seem to localise and route percolation of water flow [Pluhar 66]. They are usually due to release of strain (tension joints) [Jenning 71], but may also be shear or gravity slump joints [Pluhar 66]. The size and orientation of the joints of a given area of equal stress are influenced by lithology and topography (Pluhar 66). Pavement is best produced when bedding planes and topography are near horizontal. Inclined pavement results when the dip of beds coincide to hill slopes [Sweeting 72].

Sweeting (72) provides a description of surface karren features which is closely followed by Cowell (76) in his description of the surface karren of the Bruce Peninsula. Split karren, karmenitzas, rundkarren, and clint and grikes are the most common karren feature, on the Amabel formation (Cowell 76). Of these, clint and grike, pit karren, and karmenitzas were observed in the study area.

Clint and Grike - solution along planes of weakness (joints), also known as kluft karren [Sweeting 72]. The grikes are the widened joints while the block between are called clints. Pit

- karren
- Generally small and moss occupied pit karren are frequent on the clint block surfaces [Cowell 76].
- Rund karren
- These form under vegetation and they represent poorly developed runnels 2-3cm wide, 1-2 cm deep with rounded sides and crests [Cowell 76, Sweeting 72].
- Split karren
- Similar to grikes but developed along cracks and fissures other than joints (e.g. glacial striations). On the Bruce Peninsula they tend to run parallel to the major grike orientation [Cowell 76, Sweeting 72].
- Kamenitzas
- These are flat bottomed solution pans that form from sitting stagnant water dissolution. They are other covered with a thin layer of mineral residue [Sweeting 72, Cowell 76].

1.5 COASTAL KARST

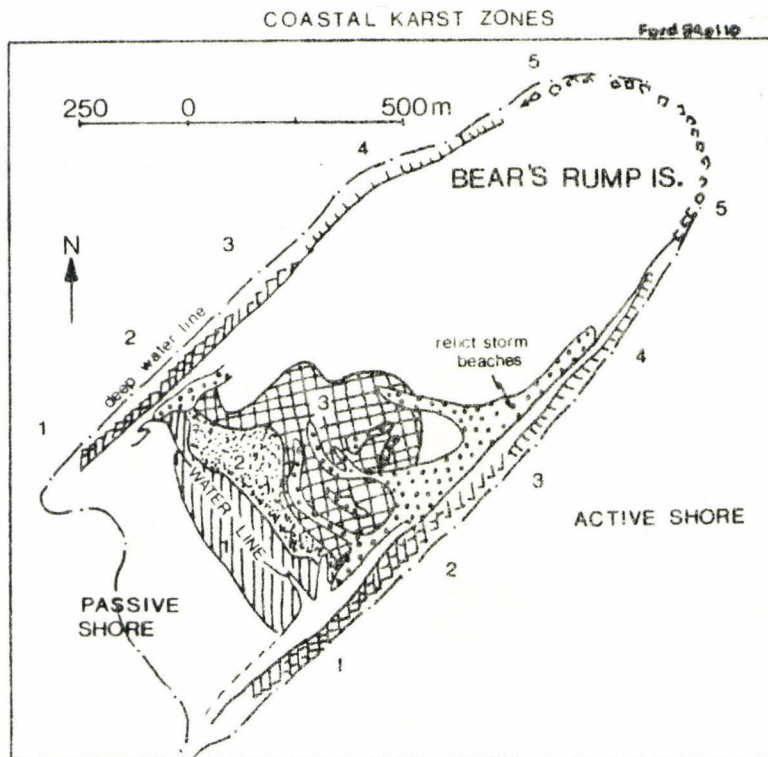
The Amabel pavement of the study area is related to coastal processes (except Dyer's Bay data). Cowell describes the shore zone environment pit karren which are prominent in these locations. They are found in high densities and associated with other karren forms (clints). Generally these pits decrease away from the shore and are structurally controlled often following joints, glacial striae or other planes of weakness. In intensely pitted areas the thin Amabel beds may be peeled off as the downward dissolution of the pits spreads horizontally along the bedding planes. This results in bedding lapies [Pluhar 66]. Littoral

pitting of the shoreline is associated with complete or partial lichen coating of the rock [Cowell 76].

The coastal karst of BRI is discussed specifically by Ford and Goodchild in a report to the Georgian Bay Island National Parks. The importance of wave action is emphasized. "Mass transfer through the boundary layer, mixing of saturated ground water, saturated lake water (Mischug-korrosion), and mechanical abrasion" are all properties of wave action which may aid in solution of local dolomite [Goodchild 84]. Fetch and prevailing wind directions influence the power of the incoming waves. Those two factors combine to produce the greatest wave energy on the NE shoreline of BRI.

Shoreline changes along the active and passive coasts of BRI produce five and three different zones respectively [Ford 84]. The zones are listed below with a more detailed description found in the Parks reports.

Active Coast



- Zone 1 - Stratigraphic top of Wiarthon member descending gently below water
- Zone 2 - Stratigraphic top of Wiarthon 1-2 m above the water
- Zone 3 - bedding plane undercut and collapsing pavement in Wiarthon Member
- Zone 4 - disappearance of pavement with cliffs of Amabel

Zone 5 - Cliffs of Amabel and Guelph Fm with sea caves at formation interface.

Passive Coasts

Zone 1 - recent littoral solution pitting offshore for several 10's meters to depths of about 1m. The joints present show little enlargement.

Zone 2 - 1-2m above water and extending several 100's m inland where grike development is more pronounced along with povened flaking and breakup which has not been removed by waves.

Zone 3 - Grass filled grikes with a shattered surface of degraded karst. The littoral pitting has been destroyed.

Ford suggests that a progressive degradation of the dolomite littoral karst can be seen in this area.

1.7 DATA ACQUISITION

Field examination of the Amabel formation took place at three locations in late August 1984. On the mainland, outcrops were sampled at Cyprus Lake Provincial Park and Dyer's Bay. The majority of this thesis, however will be derived from data collection on Bear's Rump Island. Because of the inaccessibility of Bear's Rump during inclement weather only 1-1/2 days was spent on the island. Consequently, conclusions will be made on a data base that is smaller than desired.

The sampling method on active shorelines was to map a 5m wide strip from water to treeline across the pavement. Grike orientations and dimensions were recorded within this area along with notable properties such as karren. Grike width depth and fill (rubble, dirt-soil, vegetation,

water or a combination) were recorded at one meter intervals along the grikes. In order to graphically determine point heights above water profiles were constructed along the sample strip borders. (Appendix II)

Time permitted only one sample line on the passive coast of BRI. This involved sampling the pavement from the water to treeline at 30m intervals. Each station consisted of an imaginary circle 4m in diameter. A sketch was made noting percentage vegetation, fracturing (moved (transported) or insitu (stationary) fracturing), pitting, shattering or flaking, grike orientation and dimensions, and soil and rubble depths. If a station randomly occurred where no rock outcropped the nearest exposed surface was sampled. This occurred at stations Ll-5, Ll-8, and Ll-9.

The Cyprus Lake Park shoreline is an intermediate coast with both active and passive properties. Consequently the active shore sample strip method was employed along with 1 meter square detailed karren analysis grids at 5 sites of varying heights and distances from the water.

The Dyers Bay sample site was located approximately 1km inland. A small section was mapped, in a manner similar to that of active shorelines (Appendix VII).

This thesis is a study in coastal pavement degradation on the Amabel formation outcropping near the tip of the Bruce Peninsula. Passive, intermediate, and active shorelines influence dolomite break-up to different extents. Chapter's 2 through 4 examine these controls.

CHAPTER 2.0 PASSIVE SHORELINE PAVEMENT DEGRADATION

The passive SE shoreline of Bear's Rump Island was sampled on a 30m interval from shoreline to treeline. Vegetation and grike conditions, pitting, fracturing (flaking and shatter), and soil and rubble depths were observed and subsequently ranked at each sample station. These rankings are given for each property in Table 2.0.1. Trends of pavement change are analysed under the four criteria mentioned above.

PASSIVE PAVEMENT PROPERTY RANKS **TABLE 2.0.1**

	STATION	DIST TO WATER (m)	VEG %	PITTING	SHATTER	FLAKING	GRIKE CONDITION	SOIL & RUBBLE DEPTH S	D
STORM WASH ZONE	L1-0	0	11	1	-	-	1	7	6
	L1-1	30	10	4	-	4	2	9	5
	L1-2	60	9	6	-	-	-	3	8
STORM WASH LIMIT									
TRANSITION ZONE	L1-3	90	7	7	5	-	3	1	4
	L1-4	120	8	8	4	3	4	2	2
	L1-5	150	6	8	3	5	5	6	3
PRE-TREELINE (BOUNDARY) ZONE	L1-6	180	5	2	2	4	-	4	1
	L1-7	210	4	3	1	2	6	1	10
	L1-8	240	3	5	-	-	7	6	11
	L1-9	270	2	9	6	1	-	8	7
	L1-10	293	1	8	-	-	-	5	9

2.1 VEGETATION COVER AND GRIKE CONDITION TRENDS

1 Station which shows best development of property
11 Station which shows poorest development of property

Perhaps one of the most obvious trends is that of vegetation change. In an absolute sense the vegetation (percentage) cover increased progressively from the shoreline (L1-1) to the tree line (L1-10). Stations L1-3 and L1-4 situated just beyond the storm wash limit record nearly identical values of 45% and 40% respectively. This increase in pavement cultivation mimicks overall pavement degradation inland. Biogenic acids produced from plantlife create more aggressive surface waters which percolate to and chemically attack the pavement. Intensified solution

results. The water may drain to the lake, evaporate, become used biologically, or get stored in the joints and fissures of the bedrock (subcutaneous aquifer [L. R. Beard et al 83]).

Three sub-properties of vegetation important to overall pavement condition are growth location, (association to grikes), elevation (high spots vs. gullies), and type (grass, shrubs, bushes, or trees).

Grikes are the dominant nucleus of growth, regardless of plant type or ground elevation. The expanded crack of the grike whether free from rubble (L1-0) or not serves to trap small bits of debris moved around by wave action or left by decaying plants. Thus a type of soil and moisture trap develops. Conditions are favourable for growth and the different varieties of plants are able to take root. In the storm (L1-0 to L1-2) wash zone the grikes are susceptible to wash out by incoming waves. This effectively cleans out the soil trap therefore keeping vegetation percentages low. This wash out effect is supported by the clean well defined grikes of L1-0 and L1-1 as compared to the diffuse vegetation and rubble choked grikes of L1-3 - L1-5, L1-6, L1-7. Beyond the storm limit (L1-3 - L1-10) wash out is minimal and vegetation can play a more decisive role in pavement degradation (vegetation %ages increase dramatically L1-2=17%, L1-3=45%). Grike exploitation by vegetation is demonstrated by the declining condition of the grikes beyond the storm wash limit.

At greater distances from the water grike nucleation of growth is still apparent as plants expand via crawler roots out of grikes over the clint surfaces. The densest growth still occurs along the grike.

The elevation of the pavement is important to the moisture

requirements of the plantlife. Wispy grasses, the hardest pavement plant, thrive in low ponded areas as well as on higher dry areas. They are less abundant at the dry locations due to competition of shrubs, bushes and small trees which required more dry soils respectively. Since the Amabel Fm on Bear's Rump is nearly horizontal in dip the minor inland elevation increases of the bedrock surface is due to younger beds outcropping. The biologically significant high (dry) spots are the result of underlying vegetation build-up not minor changes in pavement thickness. Therefore elevation (high spots vs gullies) is a function of botanical build up centred on the grike soil traps. Consequently plant type may reflect pavement condition. More exploited grikes further away from the shore should build up to higher elevations and host a greater quantity of dry-land shrubs, bushes, and trees.

Wispy grasses dominate the pavement vegetation shoreward at the storm wash limit where vegetal build-up is prevented by wave washout of grike soil. An occasional low shrub rooted in a grike can be found. Immediately beyond the storm limit a slight increase in shrub frequency on high well vegetated grikes was noted. At L1-3 a few small trees were observed on high spots. An important change was the introduction of moss along with grasses as the dominant form of vegetation. These mosses were not abundant in areas susceptible to storm wash. Ninety meters to 150 m from shore (L1-3 to L1-5) vegetation cover remains around 50% consisting of mainly moss and grass with minor amounts of shrubs, bushes and trees found only on dry built up grikes. This is a transition zone leading to a second major vegetation change between 150 to 180 m inland (L1-5 L1-6). This

second shift of vegetation coverage jumps from 50% grass and moss largely confined to grikes, to 80% plus, grasses, shrubs, bushes spralling out over clint surfaces, L1-6 (180m away) through L1-10 (293m away at treeline) vegetation data is summarized in table 2.1.1.

Table 2.1.1

STATION	DIST TO WATER m	OVERALL VEG%	GRASS %	SHRUB %	BUSH %	TREE %
L1-6	180	80%	60%	40%	—	—
L1-7	210	85%	40%	40%	20%	—
L1-8	240	90%	35%	50%	10%	—
L1-9	270	95%	15%	70%	15%	—
L1-10	293	100%	—	—	—	100%

The third "pretreeline" pavement zone is characterized by extensive vegetal cover of an increasingly more stable (shrubs and bushes over grasses) variety. Greater areas of dry "built up" plant debris combined with a stratigraphic upstepping are the reason for more shrubs and bushes. Build up is presently occurring in the transition zone L1-3 L1-5.

The following are the important conclusions of vegetation and grike changes inland from a passive shoreline.

- 1) grikes act as soil-moisture traps and as such are centres for vegetation growth
- 2) Shoreward of the storm wash limit grike soil may be washed out. Therefore grasses have a transient life often being removed by waves. Vegetation does not have a chance to pile up "build up"

and form a dry base from more substantial plant types.

- 3) Beyond storm wash limit there is a "transition zone" over which grass and moss dominate. Vegetation "builds up" and begins to sprawl onto clint surfaces. Stations L1-3 L1-5 (90 150m inland) - approximately 50% vegetation cover.
- 4) Moss and grass important in forming grike centred "build up" base for advanced vegetation found in "pre-treeline" or "build-up" zone
- 5) L1-6 and Inland (>180m) to L1-10 represents the "build-up zone" of high vegetation cover (>80%) and quality (less grasses, more shrubs and bushes - see table 2.1.1

2.2 PITTING TRENDS

Pitkarren are circular surface solution features which occur in strings (linear pits), groups (multiple pits) or individually (normal and micropits) (fig. 2.2.1a) Cowell [76] suggest that the karren are initiated in biologically intensified solution points centred on individual lichen growths. Linear strings of pits follow lines of weakness in the the bedrock such as microfissures or joints. Multiple pits are groups of 5-7 superimposed single pits. The distinction between micro and normal pits mainly a function of size. Micropits range from 1-3mm in diameter with an average depth of 5mm. Normal single pits show considerable variance in size. It was possible to distinguish three categories; small, medium, and large pits, on the passive sample line of Bear's Rump Island (fig 2.2.1b).

Figure 2.2.1a



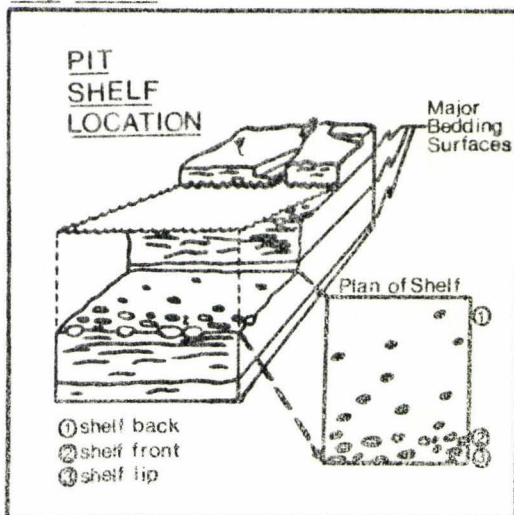
Figure 2.2.1b

	MICROPITS	SMALL SINGLE	MED SINGLE	LARGE SINGLE
Plan View				
X-section				
Dimensions				
diameter (mm)	1-3	40	10-20	15
depth (mm)	0.5	15	0.9	8-20
density	100-1000	-	6-8/100	1/1000

varieties of pits, and consequently was ranked first. A trend in pitting may be recognized when compared to the vegetation zones discussed in section 2.1.

In general pitting decreases in variety and extent through each vegetation zone. This trend is most pronounced in the storm wash zone (pit rank 1-6) and least in the transition zone (pit 7-8). Shelf location, master bedding planes, wave attack, and paleo-lake levels are important to the development of this trend. Cowell has suggested that pitting depth increases with increasing water depth. Field observations by Bob Bell on BRI indicate that the "shelf location" may be important to the development of sub-aeuous pits. Bell observed pit concentrations near the brink of pavement shelves decreasing away from the edge (fig 2.2.2)

Fig 2.2.2



Variety and extent of pitting was the criterion used for ranking the passive stations in Table 2.0.1 L1-0 at the waters edge exhibits extensive development of all four

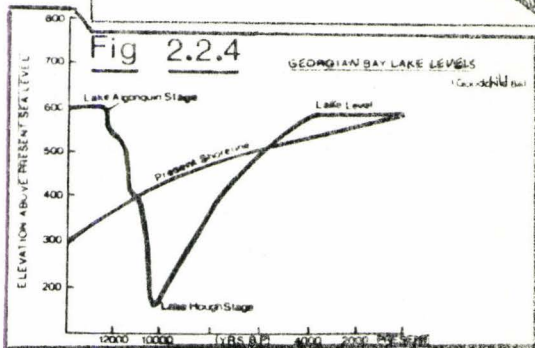
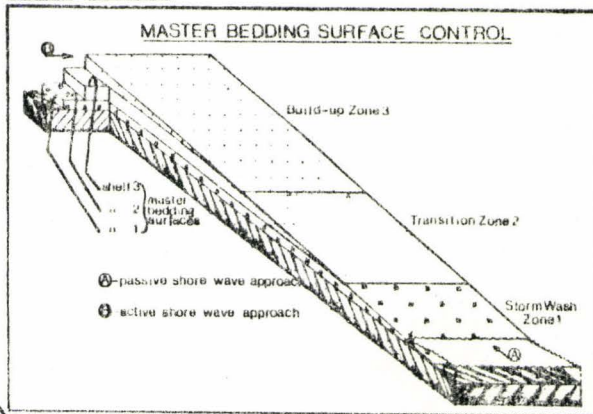
Because of quicker drop offs this observation was more apparent on the active shoreline. However it does much to explain the pitting trends observed on the passive

coast.

A geomorphologist and geologist may be at odds as to the relative importance of different bedding planes. A package of layered rocks may consist of strata observed on 3 levels. At the smallest scale, lamellae represent minor changes in the depositional environment. Silt content may increase slightly relative to the sediment below. The dolomitized rock will show fine (mm sized) dark and light banding. Bedding planes represent more abrupt changes in the depositional environment and as such form distinct breaks in the rock record. A major bedding surface (MBS) is produced by a major change in deposition, such as a period of non-deposition.

A geologist would regard lamellae and bedding plane changes in equal esteem as MBS's. To a geomorphologist, however, MBS are more important. This is due to their strong control in the breakdown of bedrock. On the active coasts of BRI grikes develop vertically downwards to MBS and then they can work horizontally. These MBS, being major planes of weakness, are likely the surfaces which initiate the shelves discussed above. The rapid rise of the pavement over short distances on active coasts (fig 2.2.3) causes MBS or shelves to outcrop in close proximity to each other. However, on the low gradient passive coast these MBS will outcrop further apart. (fig. 2.2.3) Thus it seems likely that the change from the nearshore zone to transition zone to build-up zone is in fact a stratigraphic upstepping from one MBS to the next. The pitting on these zones is greatest near the shelf edge (L1-0, L1-3, L1-6) and decreases inland to the next zone. Shatter, flaking and more aggressive soil waters

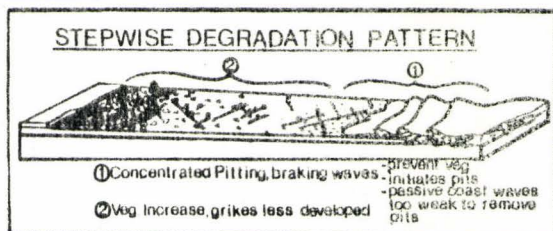
Fig. 2.2.3



initiation of pitting on these shelves.

The nearshore breaking waves would aid in pit trend development in 3 ways. First breaking waves may disrupt the saturated boundary layer next to the submerged pavement [Ford 84]. This would allow fresh aggressive water to begin pitting on point and linear weakness at the shelf edge. Secondly, storm wash would prevent nearshore vegetation build up thereby leaving the pavement relatively open and susceptible to pit karren development. Lastly, lake water swept farther inland during large storms would aid in periodic freeze than shelter and lamellae flaking of more distant pavement sections.

Figure 2.2.5



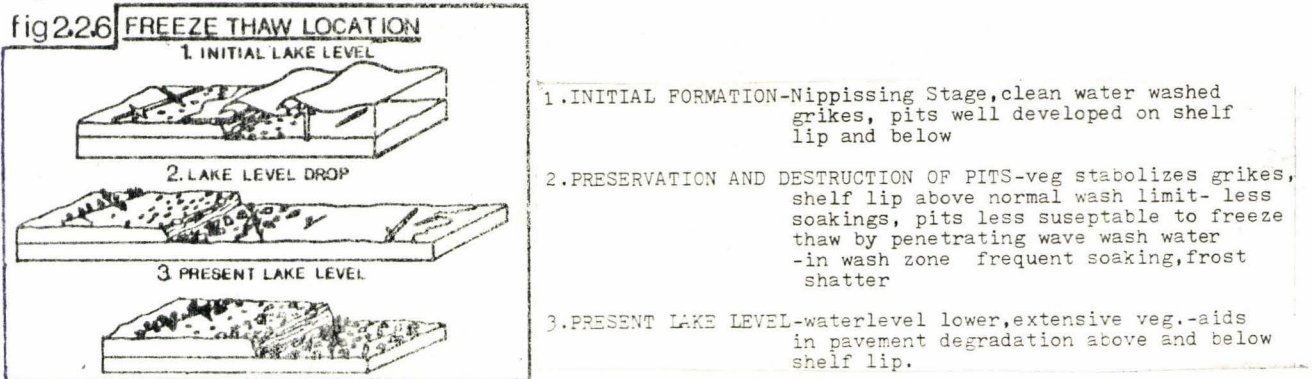
are likely responsible for this change. Another important factor are the paleo lake levels which have, varied over Geologic Time (Fig. 2.2.4).

Higher stages (Nipissing stage 4000 YBP [Goodchild 84] may have pushed the water shore contact further inland to the present transition, build up or treeline zones. This would explain the

The following conclusions may be drawn from the pit karren trend observed on the passive shore.

- 1) Pit karren variety and extent of development is related to present and former lake levels, master bedding surfaces, and shelf location.
- 2) Breaking wave location, controlled by past and present lake levels exploits linear and point weaknesses in the bedrock to develop pitkarren. Saturated boundary layer removal and bedding plane penetration may be important.
- 3) Master bedding surfaces define quasi-base levels which solution and shatter work vertically towards. Once attained lateral bedding plane solution may aid in flaking and shatter removal of bedrock.
- 4) Pit karren are best developed and preserved near the edge of present and past master bedding plane shelves. Early shatter and flaking below the shelf edge initiated destruction of the shelf bottom pavement.

Why would freeze thaw shatter and flaking occur only below the paleo-shelf edge and not also on the pit preserved lip? Fig 2.2.6 presents a possible explanation to the problem.

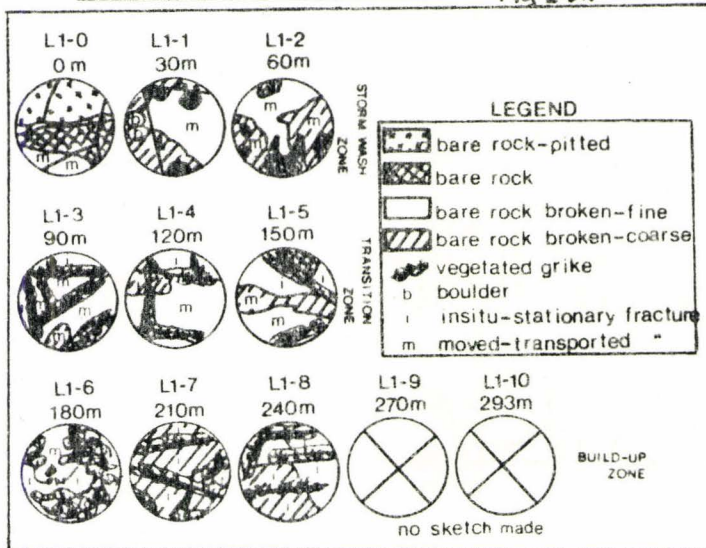


2.3 FRACTURE - FLAKING AND SHATTER TRENDS

The passive shore sample line consists of 11 stations. Sample circles, 4m in diameter were mapped into four pavement morphology characteristics; (Fig. 2.3.1) bare rock, bare rock pitted, bare rock broken fine and coarse. The last two categories were further subdivided into

moved (transported) and insitu (stationary) break up (plates A.VI.1 & A.VI.2 appendix VI). Bare rock and bare rock pitted were only observed at the waterline (station L1-0) where pavement was free of debris due to continual wave wash. Away from the immediate shoreline coarse and fine fragmented rock dominates. It is the transported or stationary nature of fracturing that is helpful in analysis.

PASSIVE SHORE MORPHOLOGY Fig 2.3.1



In the storm wash zone there is exclusively transported break-up. This is expected because of breaking waves re-arranging frost shattered material. The transition zone progresses from dominantly transported fracturing to dominantly

stationary breakup. Again this is because of wave energy dissipation. The build up, pre-treeline, zone shows almost exclusive insitu breakup. Waves have not reached this far inland since the higher lake levels of the Nipissing stage. The insitu break-up represents fracturing that has occur subsequent to earlier high lake levels. The tendency of stationary and transported break-up to change at the same boundaries as vegetation and pitting changes supports the idea of paleo-lake levels and MBS shelf control of inland pavement degradation.

Previous discussion on pitting and vegetation implied that pavement break-up should be greatest below MBS shelf edges where abundant moisture

and remnant pits would have allowed significant freeze thaw prying and shatter of the pavement. If this is the case one would expect to see fracture (shatter and flaking) increasing up to the shelf bottom, then dropping drastically as the new MBS shelf is encountered (Figs. 2.2.5, 2.2.6). This simple cyclic trend is not apparent for at least two reasons; competition between shatter and flaking, and vegetation.

Shatter and flaking are two different forms of rock fracturing (as used in this thesis). Shattering, the direct result of freeze thaw rock breakup, produces sharp angular fragments split through several lamellae or beds. Flaking, however, is due to water penetration along lamellae bedding planes. As a result thin pieces of shatter vs flaked plate-like fragments are peeled or flaked off (Plates A.VI.1 & A.VI.3 appendix VI). Those two processes seem to be in competition inland from the passive shoreline. Shattering is non-existent in the storm wash zone, whereas flaking does occur slightly at station L1-1. Shattering is responsible for more of the rock fracture through the transition zone and 60m into the build up zone. Beyond this flaking seems to dominate. The two forms of fracturing tend to confuse a cyclic trend which would be consistent with pitting and MBS shelves. Although there is some overlap of the transition and build up zone borders shattering and flaking do appear to increase (in a staggered fashion) inland. Therefore MBS shelves are not negated by the shatter-flaking pattern.

Vegetation may obscure cyclic patterns of fracturing. As mentioned previously vegetation increases continuously from shoreline treeline. There are jumps in the % of vegetation cover but the overall rooting and

growth of the various plants will aid in the break up or fracture of the pavement. Thus a continually increasing vegetation cover will tend to erase cyclic inland fracture patterns by increased root breakup in the more intact shelf front areas. This will help produce the observed quasi-linear inland fractureing pattern.

Three conclusions may be reached with regards to pavement fracturing on sample line 1.

- 1) Fracturing does not occur in a cyclic pattern due to competition between shattering and flaking, and stablizing vegetation control.
- 2) A "quasi-linear" increase in pavement fracture exists.
- 3) The dominance of moved or insitu breakup is loosely related to the storm wash, transition, and build up zones discussed in section 2.1.

Storm was zone - transported fracture

transition zone - ranges from transported dominated to stationary dominated

build up - Stationary domianted to totally stationary (pre-treeline)

2.4 SOIL AND RUBBLE DEPTHS TRENDS

Soil and rubble depth measurements were recorded at 4 circumference points and the centre of each sample station. Averages were calculated. Ranking these values from deepest (1) to shallowest (10) suggests two weak trends which support MBS shelf and paleo-lake level control of pavement degradation. These trends are inverse peak relationships, and out of phase

increases (and decreases) in soil and rubble depths (fig. 2.4.1)

Fig. 2.4.1 a emphasizes the general inverse relationship between soil and rubble depth, best expressed at peak rankings (black arrows). Rubble depths ranking higher than adjacent stations (e.g. point

Fig. 2.4.1

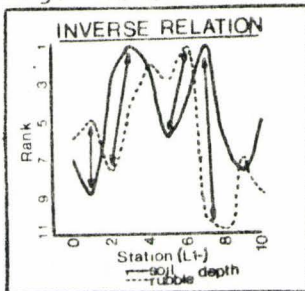
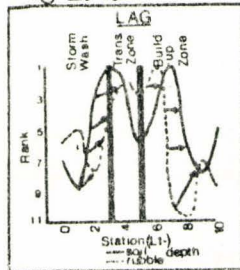


Fig 2.4.2



A) have soil depths which are lower than adjacent stations (point B). this suggests that one parameter develops at the expense of the other.

Relatively high rubble depths (L1-1 pt A) are produced by storm wash aided flaking and shattering and any soil present is washed away. A drop in the lake level allows rubble breakdown to be stabilized (first in soil trap grikes). The present waterline is a drop from higher Nippissing levels therefore transition and build up zone soils were stabilized during past water level drops. The sequence of rubble breakdown to soil is expressed as the horizontally alternating rubble and soil depth peaks of Fig. 2.4.1. Deep rubble and shallow soil, characteristic of nearshore wave wash zone, occurs at the beginning of each storm wash, transition and build up zone.

The second trend is more obscure and involves rubble and depth changes being out of phase. That is rubble (soil) depths changes seems to lag behind soil (rubble) depth changes (fig 2.4.2). The lagging property changes in the different passive shore zones. Rubble depth increases, in the storm wash zone, lags behind the soil depth increases. Incoming waves can easily sweep loose rubble further inland whereas soil trapped in grikes is hard to dislodge. Therefore rubble increases quickly at and beyond the

storm wash limit but soil depth increases before this due to grike and vegetation trapping. The transition zone shows declining soil and rubble depths again with a slower rubble depth response.

Beyond the transition zone soil depth increases lags behind rubble depth increases. Externally derived rubble and soil is not introduced to this zone. Soil therefore is developed from stationary rubble breakdown and vegetation decay. Consequently, more soil is produced from pavement debris which has been exposed to the elements for long periods of time. Past lake levels have totally submerged the island, thus pavement exposure time (since submergence) increases with elevation. This means that the passive pavement further inland has been exposed longer. Therefore soil development (i.e. soil density), which requires longer exposure time than rubble development, lags behind rubble development (depth) at any one location. This trend was reversed in the lower zones by recent wave action which penetrated and disrupted soil and rubble distributions.

Three conclusions may be drawn from the above discussion.

- 1) Observed trends were weak and unclear due to wave wash and vegetation interference.
- 2) Soil and Rubble depths show an inverse relationship of peak and trough depths. This is due to an out of phase depth change relationship discussed in conclusion #3.
- 3) Rubble and soil depth changes are out of phase. Wave action disrupts the pattern in the storm wash and transition zone causing rubble depth changes to lag inland from soil depth changes. In the build up zone the lag is reversed.

CHAPTER 3.0 INTERMEDIATE SHORELINE PAVEMENT DEGRADATION

3.1 DETAILED KARREN ANALYSIS - CYPRUS LAKE

Cyprus Lake Provincial Park represents an intermediate energy coast between the high energy active NW side of BRI and passive, low energy SE end of the island. Also, sharper and steeper cliffs are found at Cyprus Lake: Plates A.VI.4 - A.VI.8 (appendix VI) and Table A.VI.1 presents the data recorded at 5 l x 1m pavement grids in the vicinity of Cyprus Lake sample strips #1 & 2. Detailed observations at variable distances above and away from the water (K1 - K5) suggest four trends in the pavement degradation. Karren variety, surface morphology, age, and vegetation all show progressive changes away from the water. Cyprus Lake has a steep, jointed, irregular coastline. Thus certain sections will be more wave protected than others. Consequently, the absolute heights and distances of sample grids from the water are not as important as the general trends that may be extrapolated from them. A range of wave energies impact on the different sample grid locations.

As the frequency of impacting waves decreases (increasing distance from water) the variety of surface karren seems to increase. Zone K-1 (at the water line) other than minor pan development has no distinct surface solution features (Plate A.VI.4) K-2 (0.5m above, 0.5m away from the water) is also limited in the types of karren present (Plate A.VI.5). There is a straight grike, and sharp edged pan development. Grikes are poorly developed at Cyprus lake but jointing is common from the shoreline to the treeline. Thus the frequency is not as important as their form. The

grike in K-2 is straight and slightly expanded with sharp lips. Pitting is introduced in zone K-3 (1.5m above, 1.75m away), some micropits, strong single pits and worn down or "destroyed" pitting can be seen (plate A.VI.6). K-4 shows areas of dense pitting as well as more diffuse destroyed pits (Plate A.VI.7). The densely pitted area consists of micropits (diameter 1-3mm, depth 1-2mm) and single pits (1.7 diameter x .5 cm depth) which appear to line a large, previously formed pan. The greatest variety of karren was observed in K-5 (2m above, 10m away from the water, plate A.VI.8). Several vegetated grikes, rounded pits and pans, abundant destroyed pitting, and occasional (root initiated karren) were present.

This trend of increasing surface solution forms away from the water is consistent with the notion of inland pavement degradation. As more varieties of karren form, or older ones are destroyed (K-4 dense pitting superimposing on previous pan development) the overall state of the pavement declines.

The complexity of the surface morphology as examined on a meter scale seems to decrease with distance from the water. K1 at the water line has a confused surface of rough bottom pans, flat sloping areas and ledge and step zones. Some flaking due to water penetration along micro cracks of exposed joint faces may occur. Wave induced flaking along corroded planes of weakness, and the availability of fresh aggressive water may be responsible for the irregular surface. K-2 has a more simplified surface expression. Flaking has seemingly flattened off half of the grid while surface solution features are developing on the other half. Thus we have

changed from a fairly complex morphology with several surface categories to a flat grid which shows the beginnings of increased karren development. This simplification continues through K-3, K-4, and K-5. In K3 a flat morphology with superimposed pitting exists (be it micro, single, or destroyed pitting). K4 is a more unimodal surface dominated by destroyed pitting. Ultimately K5, which shows the greatest karren variety, has the simplest overall flat morphology. The greater variety and quantity of karren serve to flatten and simplify the overall morphology of the pavement.

As dolomite is exposed to the elements karst solution may occur. It is therefore reasonable to assume that surface karren will be better developed after long bedrock exposure periods. Thus the relative age of the surface rock should generally increase away from the water as does the variety of surface karren forms.

Exposure age difference between a water line and treeline sample would be far less than the resolution of isotopic dating methods. This impracticability along with high laboratory expenses made such dating procedures infeasible.

There are, however, certain observations which allow for relative dating between adjacent section of the outcrop. Pitting, karren supersaturation, and lichen cover all provide clues to the relative time the crack has been subject to wind, wave and weather. K-1 at the waterline shows 100% fresh surfaces. The minimal karren development (Rough bottom pans), lack of pitting and total absence of lichen suggest that the surface is continually being worked off by mechanical and chemical weathering. The near constant action of breaking waves supplies the necessary power to pry

up and flake off pieces of the bedrock along solution attached plains of weakness thereby exposing new bedrock. A second function of waves may be to disrupt the protective boundary layer of CaCO_3 saturated water immediately next to the dolomite. Once broken aggressive lake water could gain direct access to the dolomite resulting in dissolution. This is similar to threshold formation of scallops on cave walls for critical conduit flow with Reynolds numbers exceeding 22000 [Ford 83]. The idea of a protective thin boundary layer being disrupted by breaking waves may be important to isolated pit formation near the waterline on Bear's Rump Island.

K-2 continues to show young surfaces with no lichen growth and limited karren expressed as small developing pans. No pitting was also suggests a relatively short exposure time. K3 is a transitional grid in terms of surface age. In relative terms there exists a young, intermediate, and old exposure age zones (Table A.VI.1, plate A.VI.6, Appendix VI). The youngest exposure zone shows considerable flaking of upper lamellae, dark rock with little lichen cover and only one 'single-pit'. The intermediate exposure zone (K 3-1), however, shows destroyed (remnant) pitting, some small superimposed micro pits, and the whole zone appears to be on one bedding surface. K-3-2 the oldest exposures zone is the most extensively and deeply pitted of the three. These pits are often developed into and through destroyed pits and micropitting may be found inside them. Where K-3-2 borders on the intermediate exposure K3-1 zone several step-like levels may be found as a transition form, the higher older exposure (K-3-2) bedding plane to the younger exposure (K-3-2

intermediate) bedding level. Thus, the intermediate exposure zone has had lamellae flaked off to a lower level thereby exposing fresh (young exposure time) surfaces.

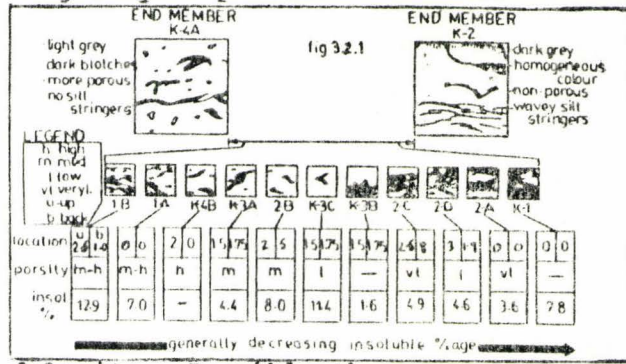
Continuing away from the water the pavement continues to show signs of longer exposure time. K4 has considerable destroyed pitting, pitting and micropits superimposed on earlier pan development. K-5 shows destroyed pitting, remnant pans, vegetation-filled grikes and extensive lichen cover. All of these properties support the general trend, of increasing surface exposure duration away from the water.

The quantity of lichen, and vegetation fill in grikes definitely increases with distance from the water. This vegetation trend is due to the biologically more stable conditions encountered beyond the direct wave attack zone. As mentioned above it is useful as a criterion of surface exposure age.

3.2 HAND SPECIMEN ANALYSIS

The dolomites at 'Cyprus' Lake are low porosity, fine grained micrites of high purity. Colour, homogeneity, porosity and the presence of dark stringers change slightly with location. At one extreme the dolomite is very light grey-white with darker inhomogeneous blotches and fairly abundant minute air vesicles, and no stringers. Dark overall homogeneous grey, low to non-porous and thin grey wavy stringers characterize the other end member. Samples from the 5 grid areas as well as the both grike sample strips on Cyprus Lake show these properties. Both extremes may be seen in the same sample but they are generally segregated into dark and light zones. In such zoned samples porosity seems to be greater in the

light areas. The small pores are a by-product of the dolomitization of the originally deposited carbonate. During diagenesis calcite is converted to



a more compact dolomite (Mg ion introduced) structure [Blatt et al 80]. The resultant loss of volume is preserved as tiny vesicles or voids in the

dolomite. Possibly these pore spaces provide traps for insolubles and thus the observed higher insoluble content. Some secondary porosity, silt-lined cracks, were also observed. Fig. 3.2.1 shows where the different samples fit with respect to the two end members.

3.3 CONCLUSIONS

The detailed karren analysis at Cyprus Lake suggests 4 pavement trends away from the shoreline. These generalized trends are not directly transferable to BRI because of different wave and shore conditions.

- 1) Increasing variety of karren due to longer exposure time of the bedrock. This allows for greater surface solutional activity.
- 2) A simplification of general surface morphology due to solutional leveling on the longer exposed bedrock.
- 3) Exposure time of the bedrock increases away from the water due to the decreasing ability of waves to flake off and dissolve older (longer exposed) dolomite surfaces.
- 4) Lichen and grike vegetation increases away from the water due to waves losing power and ability to remove the botanical build up.

4.0 ACTIVE SHORELINE PAVEMENT DEGRADATION

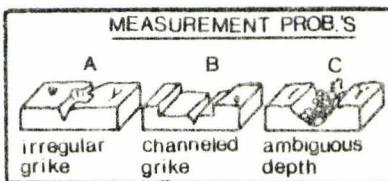
Grike widths and depths decrease inland, as the overall condition of the pavement degrades. As such, grike dimensions are assumed to be indicative of the pavement state on active shores. The degradation away from the water has been indexed by width and depth measurement on three locations of the wave attacked NW coast of BRI. The formal hypothesis to be tested is "Inland depth and width changes of grikes are due to wave attack, bedrock properties, and grike fill." Table 1.2.1 in the introduction presents the dependent and independent variables of this analysis.

This table outlines the analytical approach to the active shore analysis. (see page 4)

4.1 DEPENDENT VARIABLES: GRIKE WIDTH AND DEPTH

Width, depth and fill measurement were recorded at 1m intervals for each grike in the sample strips. Seemingly a simple procedure three problems were commonly encountered; grike irregularities, channelled grikes, and fill depth ambiguities (fig # 4.1.1)

Figure 4.1.1



Irregularities in grike form were taken as part of the measured grike and werenot actively avoided. Therefore if

a measurement station fell by chance on a particularly wide section it was still measured. Channelled grikes as depicted in Figure 4.1.1 were fairly common. Several width and depth measurements were often recorded at the

different terrace-like steps. However, for analytical purposes only the lowest grikes dimensions were used. Depth ambiguities were most prevalent in rubble filled grikes where depth measurements could vary by cm's depending on how deep the scale slid between pebbles. To resolve this problem depth was measured to a plane of equal elevation to the "general fill" level. This was estimated by eye.

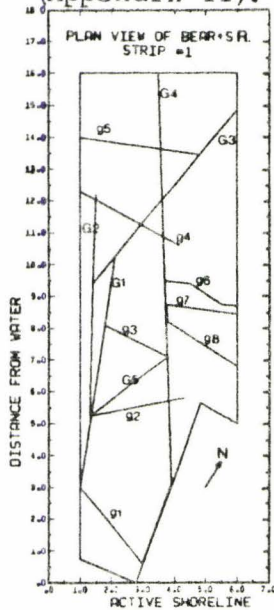
4.2 INDEPENDENT VARIABLES - Wave Attack, Grike fill, Bedrock properties

4.2 (i) Wave Attack

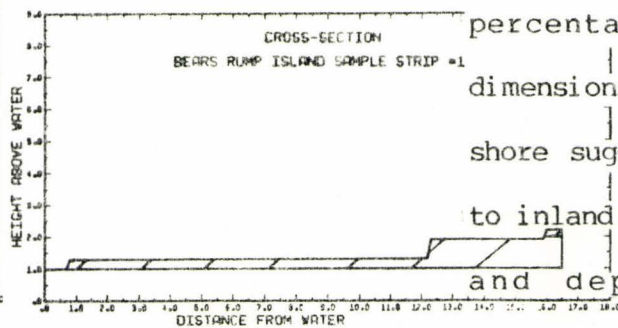
The purpose of calculating the distances inland of individual grike measurements is to form an index on potential wave attack. Higher, more distal pavement locations will be buffered from incoming waves, thus receiving less of an attack than spots nearer the waterline.

Fig 4.2.1 is a plan view and cross-section of BR SS #1. The remaining plan views and cross-sections are provided in Appendix II. Grike to shoreline distances were calculated in two ways; graphically and numerically,

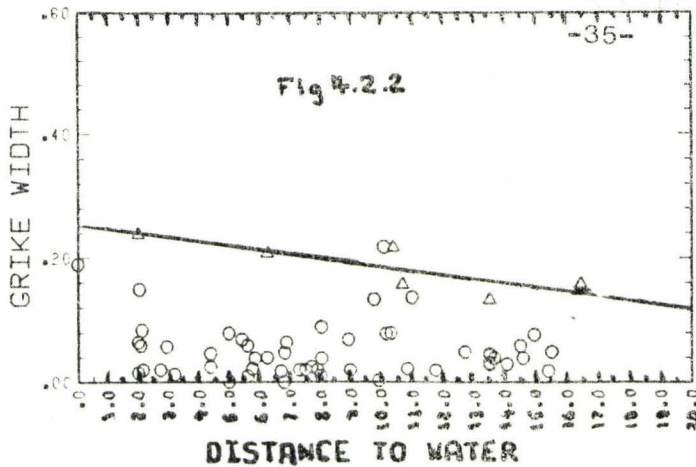
(Appendix II).



(Fig 4.2.1)



Regression analysis of grike dimensions against height and distance from the water yields very low R^2 predictive percentages. Plotting grike dimensions against distance to shore suggests possible limits to inland maximum grike widths and depths (fig 4.2.2).



Limiting data points (triangles) are isolated by eliminating noise values (circles). Regression of the refined data produces at least

square equation (line) which have very high R^2 values (Table A.1) and may be compared statistically between sites (Appendix #1). The results of those comparisons are discussed under the heading of Grike Fill.

4.2 (ii) GRIKE FILL

Grike fill ranged from nothing to rubble, dirt, vegetation, or a combination thereof. The different fill could affect grike dimensions in different ways.

Vegetation was usually combined with dirt. Acidic by-products of plant life can aid in dolomite solution thus increasing dimensional limits.

Rubble, however might armour or protect the grike walls from further solution. Pebble fill was commonly observed close to the waterline often in submerged grikes. The pebbles were rounded to angular dolomite fragments ranging in size from mm's to 10 cm in greatest diameter. These

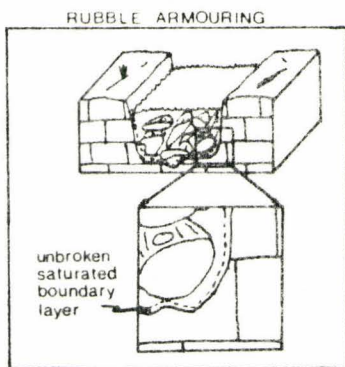


Fig 4.2.3.

obstructions form a barrier to incoming water, absorbing the impact to breaking waves. Consequently the saturated boundary layer on submerged grike walls could remain intact denying new aggressive water

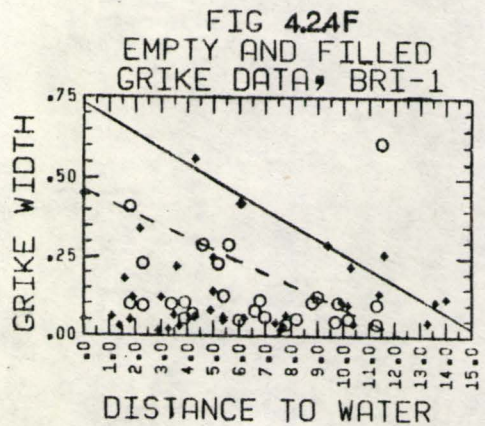
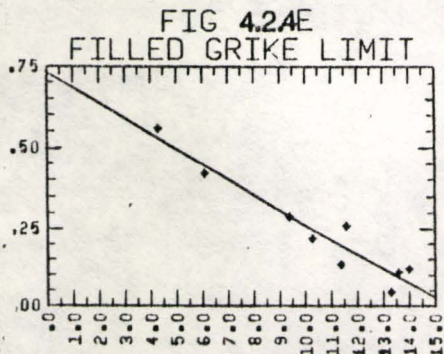
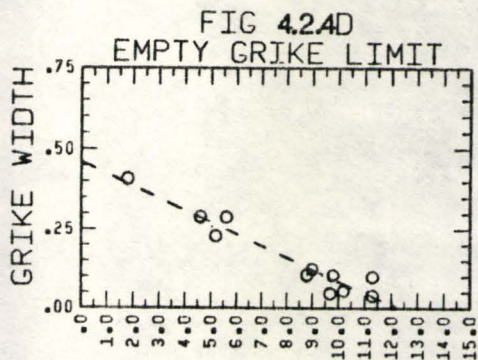
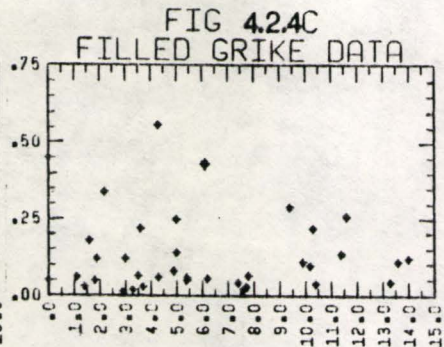
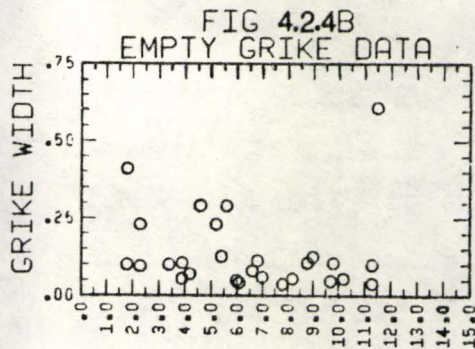
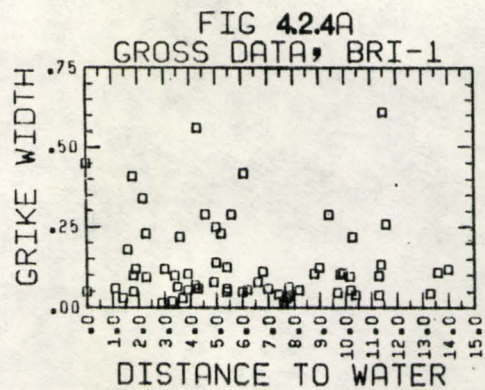
contact with the dolomite. (Fig. 4.2.3) It therefore seems reasonable that rubble armouring of grikes will effectively freeze the grike width and depth until dirt and vegetation are able to infiltrate.

All sample sites showed greater maximum grike widths for filled (vegetation) grikes than empty grikes (Appendix IV). It was possible to quantify the effect of vegetation in terms of increased width as a function of distance from shore. First, however, an explanation of filled and empty grike dimension limits is necessary. Fig 4.2.4a-f outlines the procedure of data refinement for grike widths. Fig 4.2.4 a represents all widths vs distance to water measurements for Bear's Rump sample strip # 1. This data may be subdivided into empty grike widths (fig 4.2.4 b) and filled grike widths (fig 4.2.4c). Further refinement is possible by isolating limiting values (Fig 4.2.4d) (empty), Fig 4.2.4 e (filled)) and performing linear regression to determine equations and lines of maximal grike widths (empty-dashed line fig 4.2.4d, filled-solid line fig 4.2.4 e) with distance from shore. Fig 4.2.4f summarizes the data refinement into filled and empty grike width limits. The difference between the solid and dashed line represents the increased width due to grike fill. Presumably vegetation is largely responsible as it increases water acidity thereby intensifying solution of the dolomite.

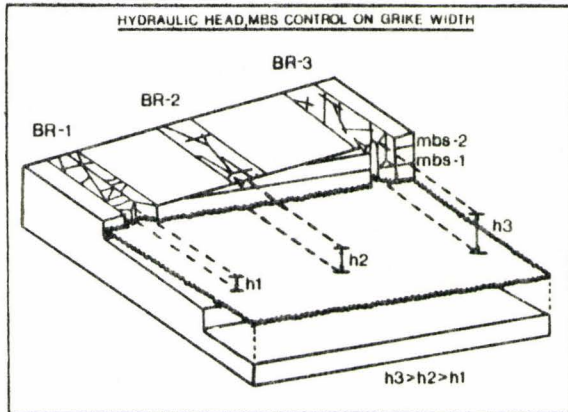
Only empty grike limits are calculated for grike depth diagrams because of fill induced inaccuracies of measurement. Cyprus Lake did have well defined depths limits, consequently grike depth vs. distance to water summary diagrams were not developed.

Table A.IV.1 (appendix IV) lists the corresponding regression line

LIMIT DERIVATION



equations for figs. 4.2.4, A.IV.1 - A.IV.4) B_1 and standard error values obtained during regression allow for statistical comparison between slopes of the dimension limiting lines. Appendix IIIA explains the procedure employed to test the null hypothesis that there is no significant difference in rate of change of inland maximal grike dimensions (slope of regression line or B_1 value) between sample sites. The null hypothesis was rejected for all width B_1 values except the empty grike widths of Cyprus Lake #1 and #2 and the filled grike limiting slopes of Bear's Rump #2 and #3. With these exceptions, the rate of change of grike dimension inland does not show statistically significant similarity between sample sites. This is reasonable for three reasons. First, hydraulic head varies between sample strips at Bear's Rump and at Cyprus lake. There is a progressive increase in the height of pavement above the water corresponding to stratigraphically younger and higher outcropping of the Wiarion member of the Amabel formation. Consequently water draining off the pavement into the lake experiences a greater drop over a shorter horizontal distance. This is reflected in potentially greater erosive and corrosive power. More aggressive fresh water passes through the bedrock to water level. The pavement surface is more removed from wave attack which may allow greater vegetation of the less frequently washed out grikes. The last cause of variation is interaction with different major bedding surfaces. Sample strip #3 on Bear's Rump is stratigraphically the highest and consequently may encounter the most major bedding surfaces. These three factors (fig 4.2.5) cause variance in the way maximal grike width's change away from the shoreline.



Comparison of grike depth limiting slopes was not possible at Cyprus Lake as no apparent limits were perceived. All three strips on Bear's Rump appear to be comparable as the

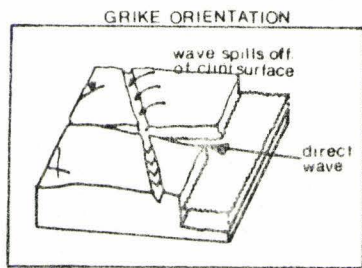
null hypothesis of no difference was not rejected (Appendix III). Why does depth change inland at a similar rate when width did not? The answer is that inland grike depths are controlled by one dominant factor: jointing. Quantifying the effect of vegetation is possible by taking the difference between filled and empty width limits (Appendix III). Table A.III.2 (Appendix III) presents vegetation effect (ve) equations. Ve is a function of the distance to water and is expressed in terms of increased grike width in meters. The values produced are maximum vegetation effects which will not always be attained. Sub-maximal noise values occur for both vegetation effects and straight grike dimensions. Such data points (non-limiting data on figs. 4.2.4, A.IV.1 - A.IV.8) occur for a number of reasons. Variable, exposure time, fill, location in the water shed all may keep the width or vegetation effect from attaining their limiting values. Exposure time of the grike is the overriding control on noise vs. limiting values. Older grikes have had sufficient time to reach maximum dimensions and show the greatest vegetation effect.

4.2 (iii) BEDROCK PROPERTIES

Joint orientations control the development and orientation of grikes. More important than the actual compass lineation is the angle the grike makes

with the shoreline. Grikes were classified as subparallel (small case "g") or sub-perpendicular (capital case "G") in the field (fig 4.2.1). Sub-perpendicular grikes would allow direct propagation of water waves whereas "g" would receive wave water that had spilled over clint surface (Fig. 4.2.6).

Fig. 4.2.6



This, too could protect a saturated boundary layer next to the grike wall as "g" grikes would not receive water in as intense a fashion as G grikes.

However, Regression of "G" and "g" widths and depths against distance from the water line produced equally insignificant R^2 values. Therefore one must conclude that the relative orientation of the grike to the shoreline does not significantly affect grike dimensions (pavement degradation) away from the water. It is possible that orientation parameter effects are overshadowed by other independent variables.

Master bedding surfaces are important to both active and passive shoreline pavements. They form major planes of weakness and may represent "quasi-base levels" of geomorphic work. The MBS represent a level at which downward percolating water becomes free to corrode horizontally. As a result grikes may work down to an MBS and then ground out as solution continues horizontally in the direction of least resistance. The MBS sets a natural limit to grike depth.

The insoluble % age by weight of the various samples is given in table A.V.1. Inspection of Bear's Rump samples indicate a range of 8.7 to 12.3 %

insolubility content. This is a rather small variance (3.6%) and could easily be due to local minor irregularities. Sample strips 1 and 2 do show increasing insolubility content away from the water based on two samples. A more detailed sampling would be necessary to statistically test this trend.

The internal description of Bear's Rump dolomites is very similar to those of Cyprus Lake. (Detailed Karren Analysis). At one extreme the dolomite is light grey, blotchy, slightly porous and does not contain any silt stringers. The opposite end has dark grey micritic dolomite without blotches abundant wavy silt stringer (see Fig. 3.2.1, p. 32). The majority of the samples taken on BR are toward the silt stringer end of the spectrum. Only sample 2B take 15m inland of sample strip #2 showed a light zone with noticeable porosity.

An interesting note is that the dark grey stringer infested dolomites at Cyprus Lake tended to have low insoluble percentages relative to the porous light grey samples. On BR, however, all the samples from the active and passive shore have higher insoluble percentages ranging from 7.4 to 12.3%.

4.3 CONCLUSIONS

Active pavement analysis has led to the following conclusions:

- 1) Vegetation fill in grikes increases width and depth dimensions by increasing the acidity of percolating waters. The resultant increased dolomite dissolution expands the grikes.
- 2) Vegetation effect in terms of added grike width is quantifiable

by comparison of filled and non filled grike width vs distance to water regressions. (Table A.III.2)

- 3) Rubble fill protects the saturated laminar boundary layer from wave disruption. Consequently the pebbles freeze grike dimensions.
- 4) Rate of change of inland grike widths (B_1 slope coefficient on regression analysis) varies between sites due to differences in hydraulic head, grike vegetation and available master bedding surfaces.

CHAPTER 5.0 SUMMARY AND CONCLUSIONS

This report has analyzed pavement degradation on passive, intermediate and active coastlines. Specific conclusions have been made throughout the text, consequently this summary will serve to re-emphasize and integrate findings from the three environments. Detailed conclusions may be found on pages 16, 20-21, 24 and 41.

The passive south-west shore of Bear's Rump Island (BRI) revealed 4 pavement zones (storm wash zone, transition zone, pre-treeline (build-up) zone, and inland forest) based on analysis of several pavement properties: vegetation cover and grike condition, pitting, fracture-flaking and shatter, and soil, rubble depths.

Three controls are responsible for such pavement zonation: master bedding surfaces (MSB), present and past lake levels, and vegetation. Master bedding surfaces are quasi-base levels that solution works vertically towards. Once attained, geomorphic work will continue in a horizontal fashion along bedding planes. This lithology determines a natural zonation tendency, because inland elevation increases encounter new MBS. Present and past lake levels are important due to the destructive nature of waves. Shoreline saturated boundary layers are broken allowing renewed dissolution and increased shatter and flaking potential. Vegetation cover destroys pavement by mechanical root action and acidification of percolating ground waters. Vegetation obliterates well defined boundaries between zones thereby producing a more progressive inland degradation pattern. The intermediate Cyprus Lake Coast was controlled largely by susceptibility to wave attack. Karren variety, exposure age and vegetation cover increased

inland levelling the pavement and producing a simplified surface morphology.

Pavement on the active north-east BRI was hypothesized to degrade (using grike dimensions as a degradational index) inland due to wave attack, bedrock properties, and grike fill. The importance of wave attack was confirmed by maximal grike dimension limits (Appendix II). Insoluble percentage and joint orientation were not found to be overly significant, however, MBS and hydraulic head (dependent on height above water) are considered important to pavement disintegration. Finally, vegetation grike fill aids pavement breakup to occur in a quantifiable way (Appendix III, Table AIII.2), while rubble fill does not.

Based on these conclusions three overriding controls on coastal pavement degradation exist:

- 1) present and past shoreline location
- 2) lithological control
- 3) vegetation influence

Past and present shorelines are more important to gentle relief passive coasts where a small waterlevel rise inundates and effects a larger section of pavement than steep active coasts.

Lithological MBS controls are important in this study area, and become more emphasized on the gentle relief coasts. Analysis of other coastal pavements should search for similar geological influence.

The effect of vegetation was best defined on active coasts using quantified vegetation effect equations (Table AIII.2). On passive pavement vegetation serves to mask and obliterate lithologically defined zones.

This thesis has demonstrated that inland degradation of coastal Amabel pavements near Tobermory strongly reflect lake level, lithologic and vegetation controls.

APPENDIX I

CHEMISTRY OF CARBONATE ROCK DISSOLUTION

The rocks of the Amabel formation studied near Tobermory are medium to thin bedded reefal and interreefal dolomite [Goodchild 84, Cowell 76]. Calcite and Dolomite are the most common carbonate minerals [Sweeting 72] with calcite being the more soluble of the two. Dolomite contains Magnesium ions which may inhibit solution rendering dolomite less soluble than calcite. A rock is considered a dolomite if 50% of the carbonate minerals are dolomite ($Mg \cdot CaCO_3$) [Ritter 78]. The dolomite of the Amabel is calcium rich with an average composition $Ca_{1.2}Mg_{0.18}(CO_3)_2$ [Goodchild 84].

The dissolution of dolomite and calcite has received considerable attention in the literature and the following is a summary of the basic principles. The main difference between dolomite and calcite is the presence or absence of a Mg^+ ions. Therefore to simplify, calcite will be used to explain the dissolution mechanism.

During its path through the atmosphere rain water absorbs CO_2 forming a weak H_2CO_3 carbonic acid [Ritter 78]. This quickly dissociates to its ionic state of $H^+ + HCO_3^-$.

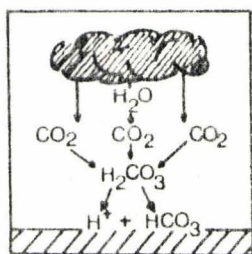
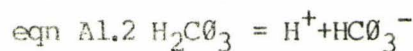


Fig A11



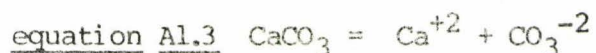
At this point the dissociated H_2CO_3 comes into contact with the Calcite. Solution proceeds in one of two ways; an open or closed system. A closed system [Drake, Ford, Gascoyne] is the result of a cut off from a

CO_2 supply once solution has began. Equilibrium or open system solution [Drake et al] is possible when activated water is continually in contact with air during CaCO_3 dissolution [Sweeting 72]. The later case is capable of much more solution due to larger concentrations of dissolved CO_2 .

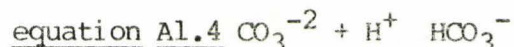
The more CO_2 dissolved the more acidic the rain water, resulting in greater dissolution. The equilibrium dissolved CO_2 concentration increases with the partial pressure of CO_2 (PCO_2) in the air [Jenning 71]. Thus, for increased dissolution of calcite a high PCO_2 is desirable. In closed systems water is only subjected to atmospheric CO_2 after which it is cut off from an air supply. The normal maximum dissolution potential for CO_2 devoid water without CO_2 is only 14 ppm (Sweeting 72).

In an open system the air supply is not cut off from the water once dissolution has begun. Exposure to soil air (which concentrates dissolved CO_2 thereby creating higher PO_2) resulting in water more saturated with CO_2 . This combined with "biogenic CO_2 " produced by microbiological decomposition of vegetated matter greatly intensifies dissolution of the carbonate bedrock [Ritter 78]. The equation 1.2.2 is pushed to the right and more H^+ ions become available.

Calcite dissociates into Ca^{+2} and CO_3^{-2} ions (equation A.1.3 [Sweeting 72]).

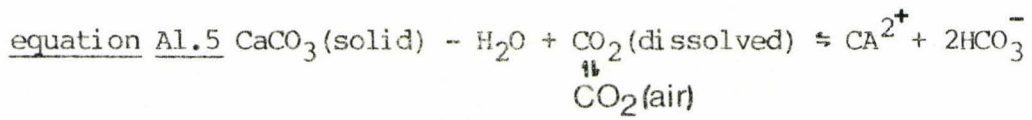


The CO_3^{-2} ions instantly combines with the H^+ in the water to produce bicarbon ions (equation 2.1.4)



The result of this reaction is to leave a higher concentration of Ca^{+2} ions. To equilibrate, more limestone is dissolved and more CO_3^{-2} ions are produced. In effect the dissolution process is perpetuated as long as there are available H^+ to remove the CO_3^{-2} from solution [Jenning]. The result is a much larger capacity of calcite dissolution in open systems.

The overall reaction is:



APPENDIX II GRIKE MEASUREMENT STATION LOCATION

a) Graphical Method

Vertical and horizontal distance of grike measurement stations from the water could be determined by measuring plan and cross-sections of the various sample strips (Fig. All.1 a + b).

Fig. All.1a

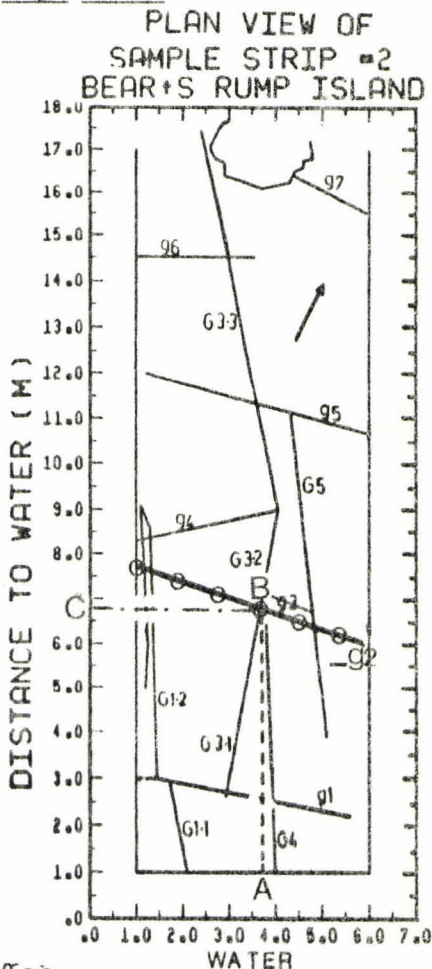


Fig. All.1b

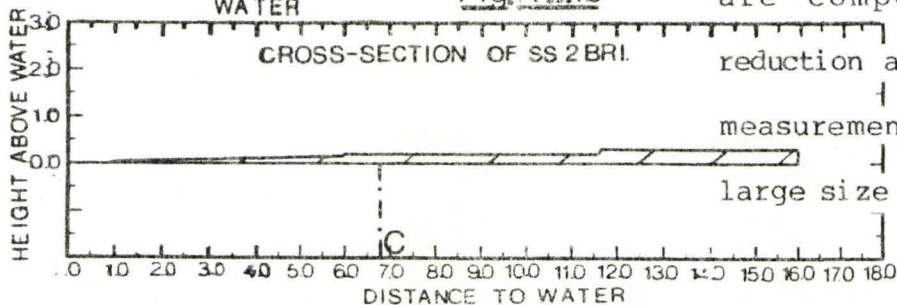


Fig. All.1a demonstrates graphical station estimation using the waterline as a reference. Shoreline sub-parallel grike g2 (heavy black line) was measured at 1 meter intervals (circles mark stations). A line was constructed and measured, at scale (dashed AB), to determine horizontal distance to the water.

By following line BC (dot-dash) to the y axis scale and then transferring to the x axis of fig. All.1b elevation above water was determined.

There are two sources of error to this method, First, inaccuracies of field mapping are compounded by scale reduction and inconsistent map measurements. Because of the large size difference between

reality and figs. AII a + b oversimplification is unavoidable. Consequently, estimation accuracy is compromised at the original mapping stage and during graphical measurement. Secondly, an irregular coastline such as BRI strip #3 (Fig. AII.4) makes it difficult to decide upon a proper reference line. This was overcome by estimating a general shoreline trend, disregarding small indentations and protrusions. The sample strip boarderlines were constructed perpendicular to the general reference trend. Thus graphical measurements were made parallel to these boundaries.

b) Numerical method

Numerical calculation of station location afforded more accurate results for two reasons. In graphical estimation field data was plotted and then measured. Numerical calculation used field data directly avoiding any secondary sources of error. Secondly, numerical manipulation allows estimation to a tenth of a meter. Graphical methods were not this precise. Consequently the numerical technique (below) was the main method of station location.

$$\text{equation AII.1} \quad \text{H.D.} = [\sin (\text{angle A} - \text{angle B}) \times D] + K$$

H.D. - horizontal distance to water

angle A - angle of general shore orientation

angle B - angle of grike orientation

D - distance (meters) along grike from starting point at which measurements were first made

K - constant - starting distance of grike away from the shoreline (parallel to sample border strips).

Fig.A11.2a

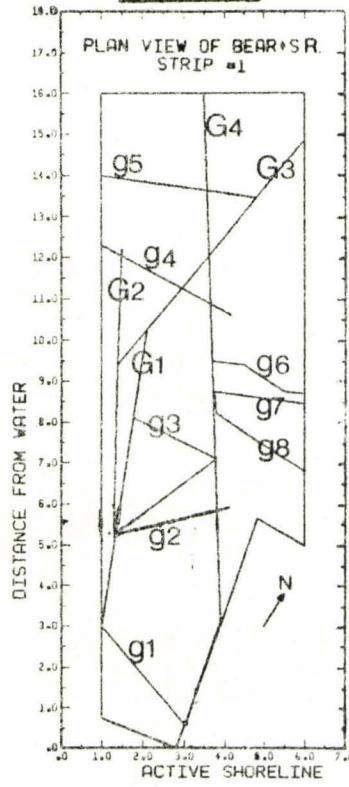


Fig.A11.2b

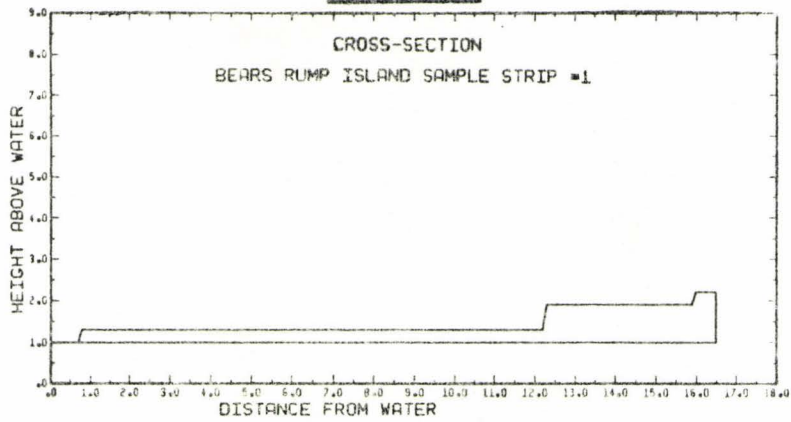


Fig A11.3a
 PLAN VIEW OF
 SAMPLE STRIP #2
 BEAR'S RUMP ISLAND

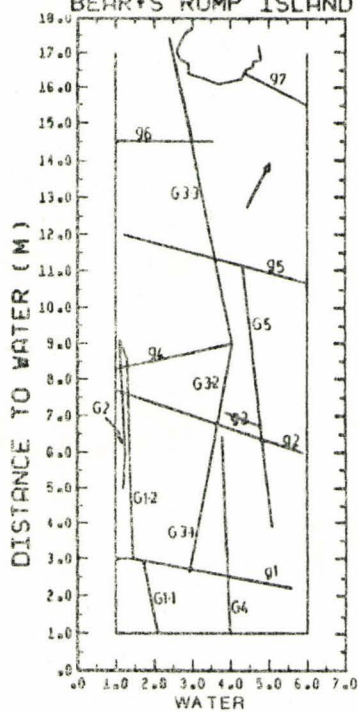


Fig A11.3b

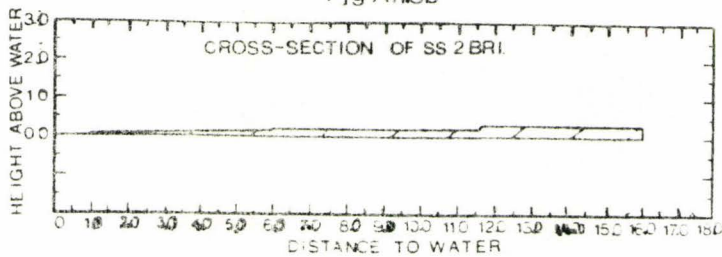


Fig.A114a

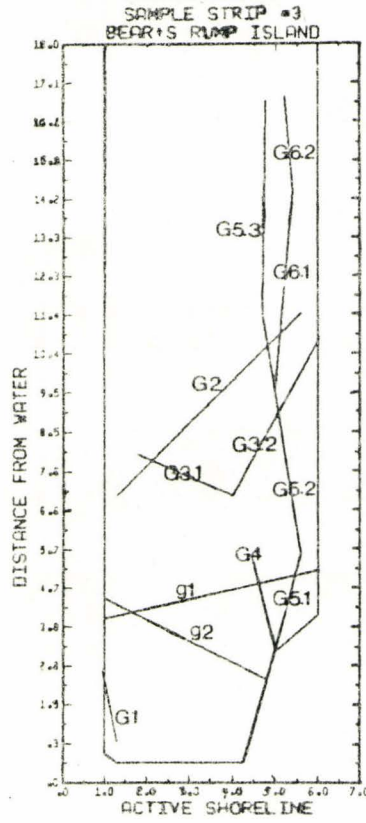


Fig.A114b

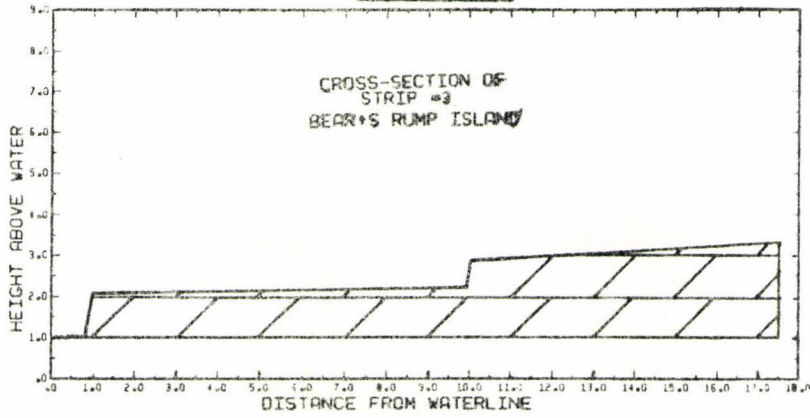


FIG. A115

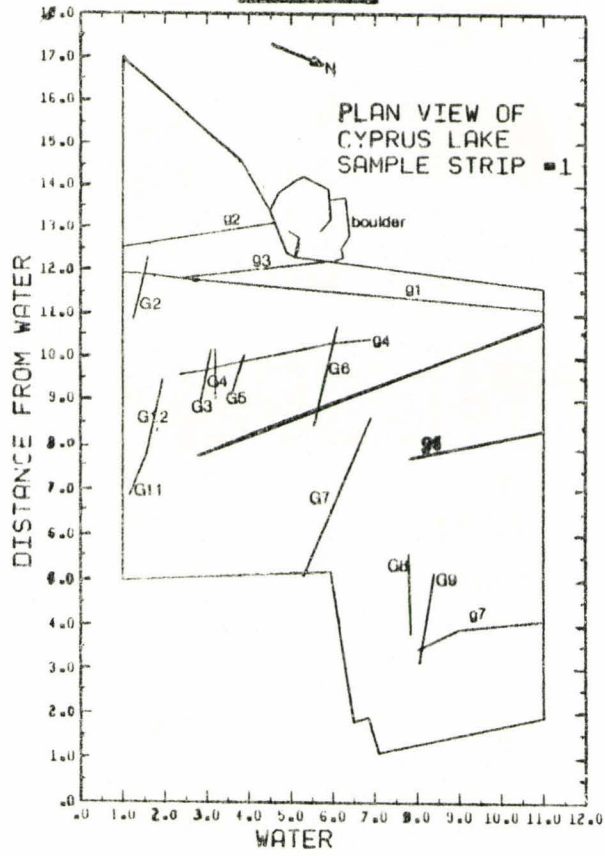


FIG. AII.6a

PLAN VIEW OF CYPRUS LAKE SAMPLE STRIP #2

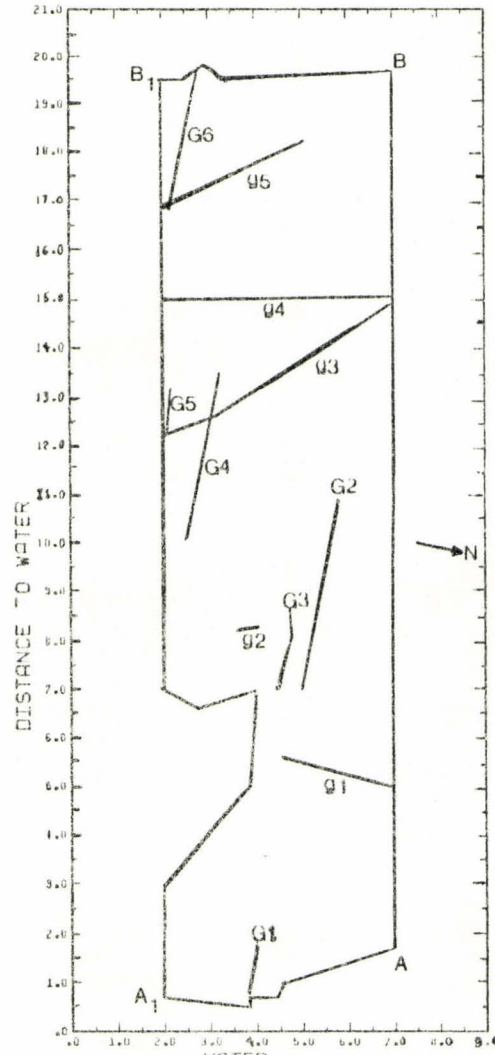
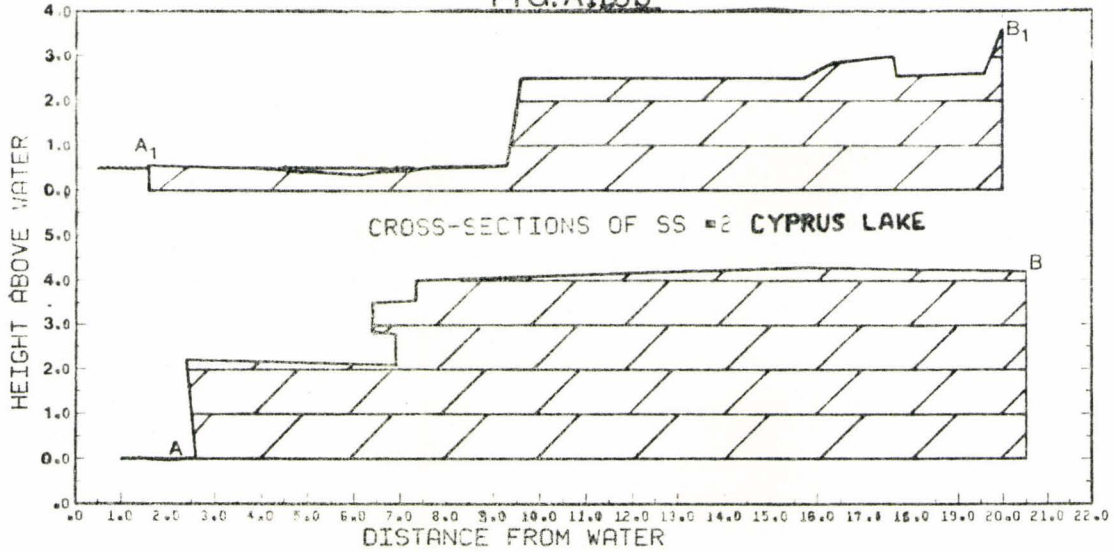


FIG. AII.6b



APPENDIX III

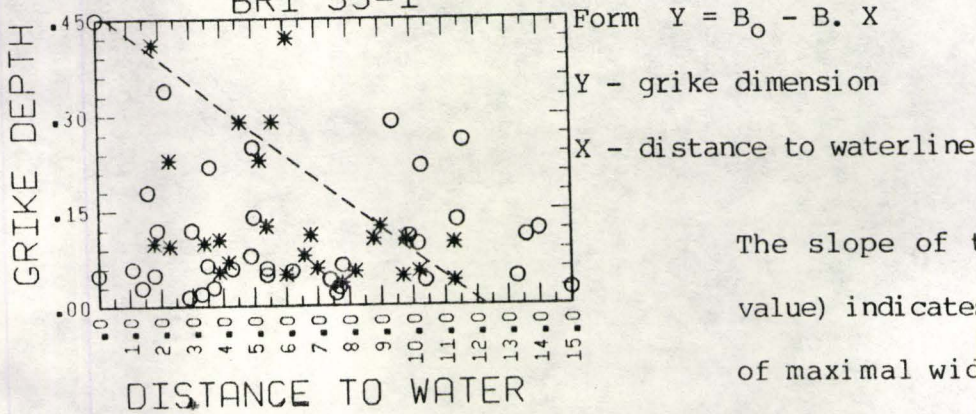
A STATISTICAL COMPARISON OF GRIKE DIMENSION CHANGE BETWEEN SAMPLE SITES

Grike widths (depths) decrease inland from the shoreline. Graphical and numerical expressions of dimension regression analysis depict maximum dimension limits as a function of distance to waterline. (fig III-1 and equations III-1, I-2)

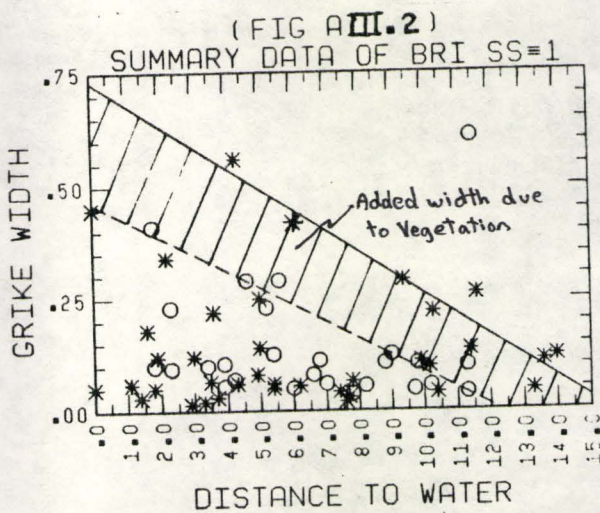
Figure III-1

Eqn III-1 $W = .463 - .0377 \text{ Dist}$

(FIG A III.1)
SUMMARY DATA DEPTHS III-2 $D = .325 - .0222 \text{ Dist}$
BRI SS=1



The slope of these lines (B_1 value) indicates rate of change of maximal width (depth) away from the water. A statistical



comparison of B_1 values will determine if there is no significant difference in rate of change of inland grike dimensions between sample locations. This analysis has been performed for width and depth measurements taken from 3 active shoreline strips on

Bear's Rump Island and two at Cyprus Lake. Sample strips Bear's Rump #1 and #2 will be used as an example to explain the procedure.

1.0 Problem Definition

a) Research and Null Hypothesis

H_1 : $B_1(1) \neq B_1(2)$ Rate of change inland maximal grike width is
 : $B_1(2) \neq B_1(1)$ not the same between BRSS #1 and BRSS#2

H_0 : $B_1(1) = B_1(2)$ There is no significant difference in rate of
 : $B_1(2) = B_1(1)$ change of inland maximal grike width
 between BRSS#1 and BRSS#2

b) Level of significance

$$= 0.05$$

a non-directional two-tailed test.

II Test selection

a) scale of measurement - grike width is measured at recorded distances from the water. The waterline is a reference base level. Therefore measurement is on a ratio scale.

b) Sample size

The sample size varies between strips. It corresponds to the # of grike dimensional measurements used to estimate the limit.

<u>Width's</u>	Empty grike	Filled Grike
BR SS1	N = 11	N = 9
BR SS2	N = 5	N = 6

BR SS3	N = 5	N = 7
<u>DEPTHS</u>	Empty grike	
BR SS1	N = 5	
BR SS2	N = 3	
BR SS3	N = 6	

c) Test selection

Significance tests of B_1 uses the standard errors of the regression coefficients and grike width. Those are calculated from the standard deviation of data points about the regression line. The standard deviation equals the root of unexplained variance, the variance of grike measurements about the regression line [Norcliff].

Student t is calculated by eqn I-3

$$\text{Eqn (A1-3) } t^* = \frac{B_1(1) - K}{Sb_1}$$

K = slope coefficient from the limiting regression equation of the comparison sample trap

Sb_1 = standard error for B_1 (slope coefficient)

II CRITICAL t

Degrees of freedom are determined by eqn (I-4)

$$\text{eqn (I-4) } D. F = N_1 + N_2 - 4$$

Therefore the critical t for a two tailed to test at a significance level of 0.05 is

$$t (N_1 + N_2 - 4), \frac{0.05}{2}$$

H_0 is reject if $t^* > t (N_1 + N_2 - 4)$

IV Computation

Regression Equations

Ho: B_1 (BR1) = B_1 (BR2) BR1 W = 463 - 1037 (Dist) N=11

B_1 (BR2) = B_1 (BR1) BR2 W = .0959 - .012X (Dist) N=5

$$\begin{aligned} t^* \text{ BR1} &= \frac{B_1(\text{BR1}) - B_1(\text{BR2})}{Sb_1(\text{BR1})} \\ &= \frac{(.0377) - (-.012)}{.003512} \\ &= 7.32 \end{aligned}$$

$$\begin{aligned} t^* \text{ BR2} &= \frac{B_1(\text{BR2}) - B_1(\text{BR1})}{Sb_1(\text{BR2})} \\ &= \frac{(-.012) - (-.0377)}{.001185} \\ &= 21.69 \end{aligned}$$

$$t(N_1 + N_2 - 4, \frac{0.05}{2})$$

$$t_{12, \frac{0.05}{2}} = 2.179$$

$T^* \text{ BR1}$ and $T^* \text{ (BR2)} > t$ Therefore Ho rate of change of maximal inland grike width is not significantly the same between BRSS#1 and BRSS#2.

TABLE AIII.1 a & b lists the conclusions for the other sample strip comparisons.

TABLE AIII.1A GRIKE WIDTH'S

<u>Locals</u>	<u>Dimensions</u>	<u>Grike</u>	<u>Null hyp</u>	<u>t*</u>	<u>T critical</u>	<u>Conclusion</u>
BR SS #1 & BR SSS #2	Width	empty	$B_1(B_{(2)}) = B_1(BR_2)$	7.32	2.179	Reject Ho
$B_1(B_{(2)}) = B_1(BR_1)$			21.69	Reject Ho		
BR #1	Width	empty	$B_1(B_{(1)}) = B_1(BR_3)$	4.76	2.179	Reject Ho
BR #3			$B_1(B_{(3)}) = B_1(BR_1)$	5.59		Reject Ho
BR #2	Width	empty	$B_1(B_{R(2)}) = B_1(BR_3)$	7.60	2.447	Reject Ho
BR #3			$B_1(B_{R(3)}) = B_1(BR_2)$	3.02		Reject Ho
CYP 1	Width	empty	$B_1(C_{Y(2)}) = B_1(CY_2)$	0.866	2.365	Do not Reject Ho
CYP 2			$B_1(C_{Y(2)}) = B_1(CY_1)$	0.055		Do not Reject Ho
BR #1	Width	Filled	$B_1(B_{R(1)}) = B_1(BR_2)$	7.66	2.201	Do not Reject Ho
BR #2			$B_1(B_{R(2)}) = B_1(BR_1)$	17.43		Do not Reject Ho
BR #1	Width	Filled	$B_1(B_{R(1)}) = B_1(BR_3)$	7.81	2.179	Do not Reject Ho
BR #3			$B_1(B_{R(3)}) = B_1(BR_1)$	37.53		Do not Reject Ho
BR #2	Width	Filled	$B_1(B_{R(2)}) = B_1(BR_3)$	0.32	2.262	Do not Reject Ho
BR #3			$B_1(B_{R(3)}) = B_1(BR_2)$	0.69		Do not Reject Ho
CYP 1	Width	Filled	$B_1(C_{Y(1)}) = B_1(CY_2)$	4.09	2.306	Reject Ho
CYP 2			$B_1(C_{Y(2)}) = B_1(CY_1)$	3.985		Reject Ho

TABLE AIII.1B Grike Depths

<u>Locals</u>	<u>Dimensions</u>	<u>Grike</u>	<u>Null hyp</u>	<u>t*</u>	<u>T critical</u>	<u>Conclusion</u>
BRSS #1	Depth	Empty	$B_1(B_{R(1)}) = B_1(BR_2)$	1.57	2.262	Do not Reject Ho
BRSS #2			$B_1(B_{R(2)}) = B_1(BR_1)$	1.48		
BRSS #1	Depth	Empty	$B_1(B_{R(1)}) = B_1(BR_3)$	1.78	2.179	Do not Reject Ho
BRSS #3			$B_1(B_{R(3)}) = B_1(BR_1)$	0.69		
BRSS #2	Depth	Empty	$B_1(B_{R(2)}) = B_1(BR_3)$	1.34	2.571	Do not Reject Ho
BRSS #3			$B_1(B_{R(3)}) = B_1(BR_2)$	0.55		

B/ Regression equations define limits of maximal inland grike widths for filled and non-filled grikes on Bear's Rump Island. The difference between them represents the effective width due to fill. Acidifying vegetation is likely the cause of larger filled grike widths. Sample strip #1 equations (AIII5, AIII6) demonstrate this method of quantifying the effect of vegetation on grike width if a given distance from shore.

eqn (AIII5) filled grike width limit $w = .731 - .047 \text{ Dist}$

Eqn(AIII6) empty grike width limit $w = .463 - .0377 \text{ Dist}$

Eqn of vegetation effect $ve = .268 - .01 \text{ Dist}$ (AIII7)

The effect of vegetation in terms of increased width of grike in meters at various distances away from the waterline for Bear's Rump Island is:

$$ve = .268 - .01 \text{ Dist}$$

Table I 2 presents similar equations for Bear's Rump Sample Strips 2 and 3.

Table AIII.2 Vegetation Effect

<u>Location</u>	<u>Limiting Regression Equation</u>		
	<u>filled grike</u>	<u>non filled grike</u>	<u>Vegetation effect</u>
BRSS#1	$w = .731 - .047 D$	$w = .463 - .0377 D$	$Ve = .268 - .01 D$
BRSS #2	$w = .253 - .00659D$	$w = .102 - .0131 D$	$Ve = .151 - .00651 D$
BRSS #3	$w = .187 - .00583D$	$w = .142 - .0163 D$	$Ve = .045 - .01047 D$
CYP #1	$w = .104 - .00963D$	$w = .0194 - .00162 D$	$Ve = .0846 - .00801 D$
CYP #2	$w = .429 - .00215D$	$w = .0545 - .00326 D$	$Ve = .3745 - .01824D$

w- width
D- depth

APPENDIX IV GRIKE DIMENSION VS. DISTANCE TO WATER

Fig. AIV.1 through AIV.5 and AIV.6 - AIV.8 respectively are summary diagrams of width and depth dimensions against distance to water. Derivation is explained in the text (pgs. 36 - 37). The hashed regions in figs. AIV.1 - AIV.5 represent the added grike width due to vegetation effect (see Appendix IIIB for discussion of vegetation effect).

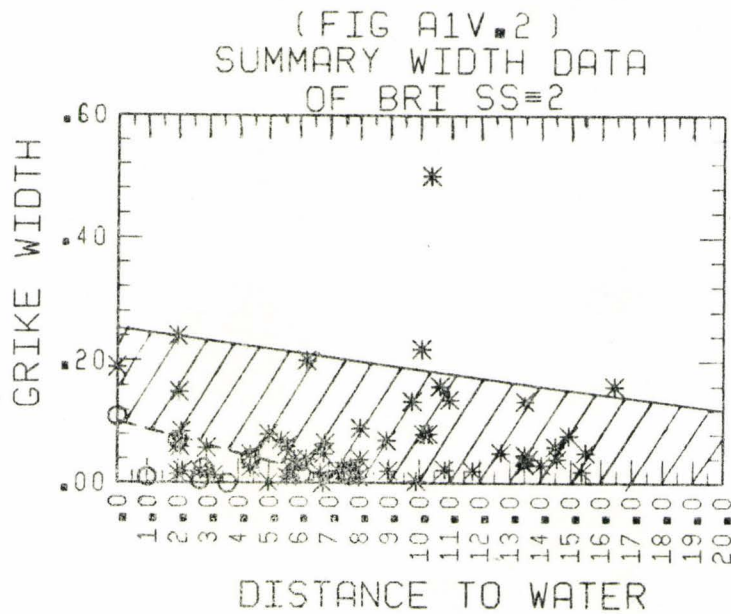
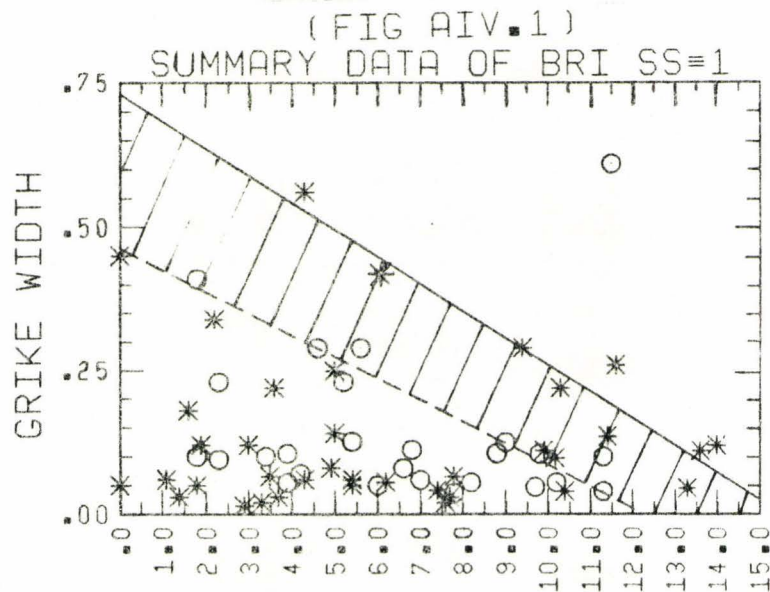


(FIG AVI.3)
 SUMMARY WIDTH DATA
 BRI SS=3

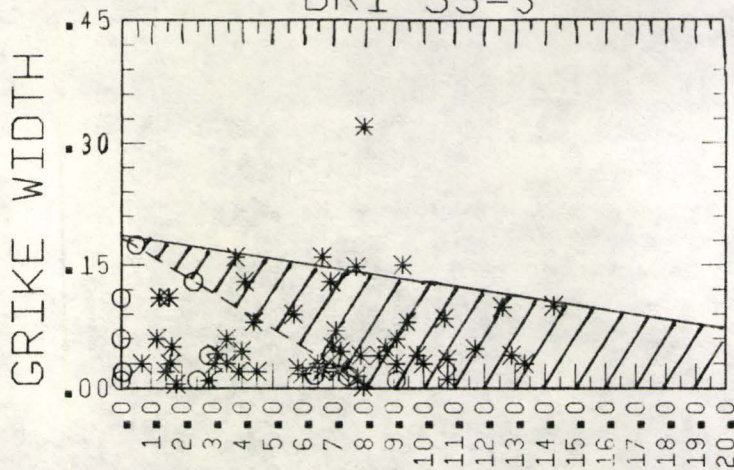
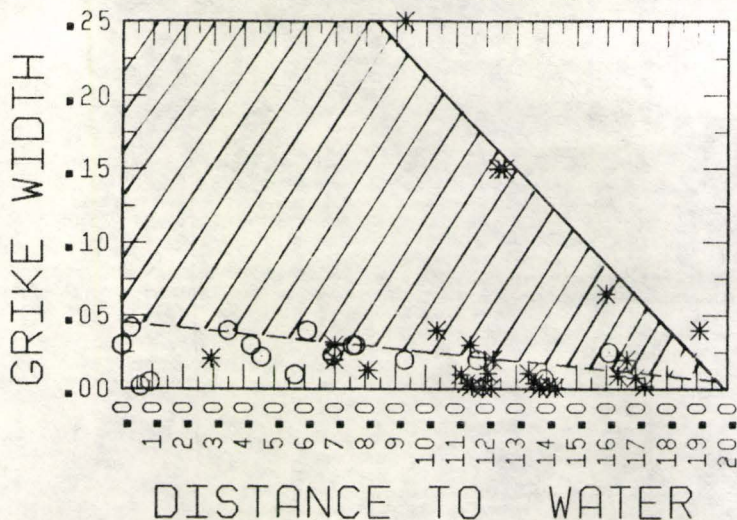


(FIG AVI.4)
 SUMMARY WIDTH DATA
 CYP L. SS=2



EMPTY GRIKE DATA VALUES	-----
FILLED GRIKE DATA VALUES	-----○-----
EMPTY GRIKE LIMITING DIMENSION (WIDTH OR DEPTH)	-----*
EMPTY GRIKE LIMITING DIMENSION (WIDTH OR DEPTH)	-----○-----

(FIG A VI . 5)
 SUMMARY WIDTH DATA
 CYP L . SS=1

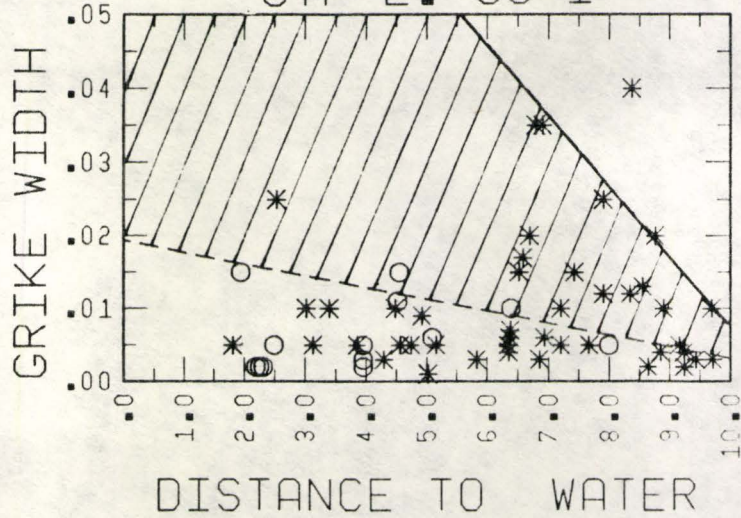


(FIG A IV . 6)
 SUMMARY DATA DEPTHS
 BRI SS=1

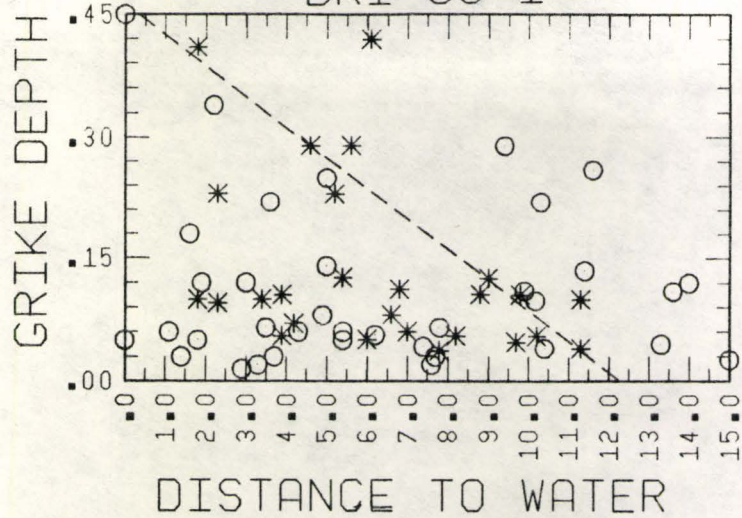


(FIG AIV.7)
 SUMMARY DATA DEPTH
 BRI SS=2

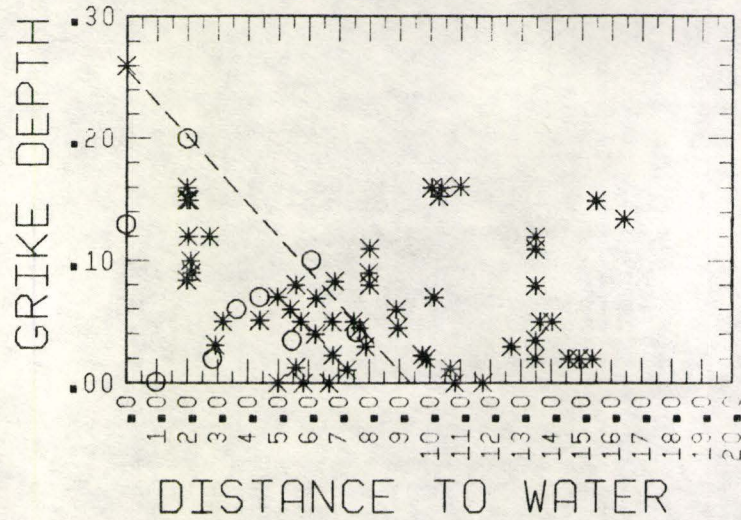
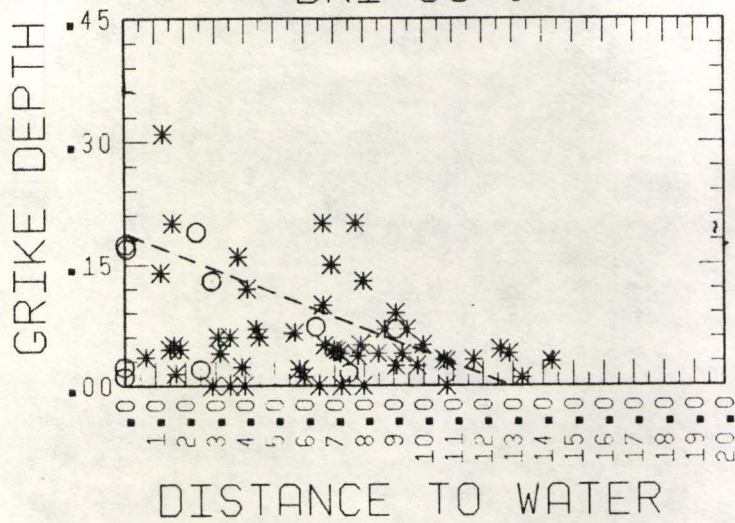


(FIG AVI.8)
 SUMMARY DEPTH DATA
 BRI SS=3



APPENDIX V DETERMINING INSOLUBLE PERCENTAGE

Several sections in the text (pgs.31-32,41) refer to insoluble content. This property was determined by dissolution of various dolomite samples collected at Bear's Rump, Cyrus Lake and Dyer's Bay. The procedure is outlined below and Table AV.1 summarizes the results.

Method

- 1) Samples were cut such that all weathered surfaces were removed.
- 2) Samples were oven dried for 24 hours and then set in the lab until a reference fragment's weight stabilized with the atmospheric moisture (Fig. AV.1).
- 3) Samples of interest were weighed and submerged in 9 M HCl until dissolved (2 days). Insoluble residue remained.
- 4) Solvent and residue were filtered using 40 and 42 grade filter paper. Beakers were filtered and contents filtered three times with 3M HCl to ensure that all insolubles ended up on the filter paper.
- 5) Filter paper was oven dried for 24 hours and weighed after a reference filter equilibrated with laboratory air moisture (fig. AV.2).
- 6) The difference between residue weight and initial sample weight was calculated as an insoluble percentage (Table AV.1).

FIG. AV.1

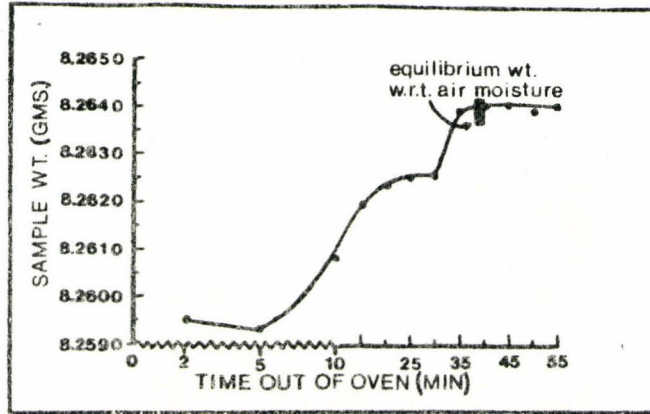


FIG. AV.2

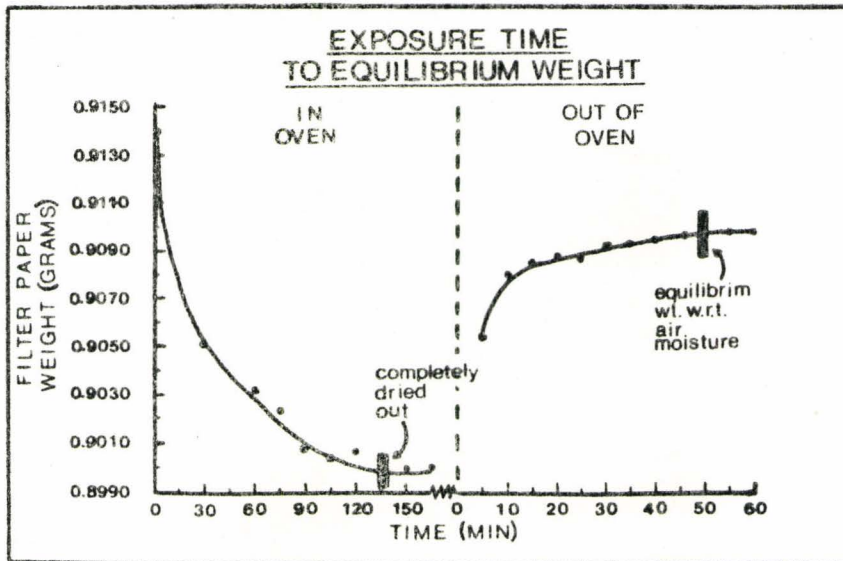


TABLE AV.1

SAMPLE	LOCATION	INITIALWT (g)	FILTER P. WT.	P. FiP&RESIDUE	RESIDUE WT.	% INSOL
BR1A	Waterline	5.1810	1.0751	1.5517	0.4766	9.2
BR1B	15 m back	5.6250	1.0689	1.7617	0.6928	12.3
BR2A	Waterline	7.0956	1.0659	1.6850	0.6191	8.7
BR2B	15 m back	3.6780	1.0660	1.4560	0.3900	10.6
BR3A	Waterline	3.5370	1.0891	1.4735	0.3844	10.9
BR3B	15 m back	4.4556	1.0533	1.5307	0.4774	10.7
L1-5	150 m back	7.9320	0.9705	1.657	0.6661	8.40
L1-6	180 m back	6.1835	0.9195	1.643	0.7031	11.37
L1-7	210 m back	3.7195	0.9162	1.375	0.4384	11.79
L1-8	240 m back	3.9976	0.9444	1.372	0.4072	10.19
L1-8b	240 m back	8.2640	0.9781	1.609	0.6105	7.39

APPENDIX VI PLATES FROM TEXT

Plates AVI.1 through AVI.9 are photographs referred to throughout the text. A brief description along with the corresponding text pages is found beneath each plate.



Plate AVI.1

-coarse moved (transported) break-up
fracture, BRI passive coast
-shattered rock, reference page 22



Plate AVI.2
-shattered insitu (stationary) break-
up fracture, BRI passive coast
-reference page 22



Plate AVI.3

-flaked rock fragments, BRI passive coast
-reference page 23

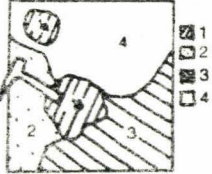
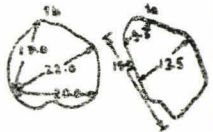




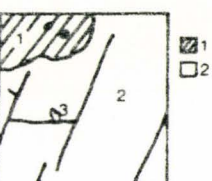
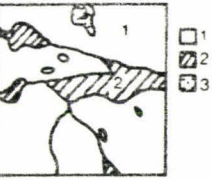
DIST AWAY FROM WATER	DIST. ABOVE WATER	INSOL. %	DIAGRAM	INDIVIDUAL CHARACTERISTICS															
K1 0	0	7.8		1 rough bottom pans 	2 flat sloping surface 	3 high rough area ridge hts 0-13 0-10 ridge lengths 21-0 22-0	4 remnant pitting 												
K2 0.5	0.5	3.4		1 flat and flakey - flat, minor flaking - no pitting - grike width 0.2-0.5 cm depth 10-20 cm orientation 105°	2 step and pan - curved features with sharp edges - no pits	3 pan - mini-pans <table border="1" data-bbox="1562 591 1709 656"> <tr><td>1</td><td>2</td><td>3</td></tr> <tr><td>23</td><td>16.5</td><td>12 cm</td></tr> <tr><td>26</td><td>13.5</td><td>10</td></tr> <tr><td>19</td><td>12.5</td><td>8.5</td></tr> </table>	1	2	3	23	16.5	12 cm	26	13.5	10	19	12.5	8.5	
1	2	3																	
23	16.5	12 cm																	
26	13.5	10																	
19	12.5	8.5																	
K3 1.75	1.5	1-1.0 2-4.4 3-11.4		1 intermediate surface - whole area on one bedding plane - a few small micropits	2 old surface - highest, shows most and deepest pits - destroyed pits present - strong lichen cover	3 young surface - rock dark with little lichen cover - only 1 pit - flaking apparent	4 pits typical pit dimensions <table border="1" data-bbox="1562 818 1709 899"> <tr><td>1</td><td>2</td><td>3</td></tr> <tr><td>7.5</td><td>5.0</td><td>5.0</td></tr> <tr><td>5.5</td><td>3.5</td><td>3.5</td></tr> <tr><td>2.0</td><td>1.8</td><td>1.0</td></tr> </table>	1	2	3	7.5	5.0	5.0	5.5	3.5	3.5	2.0	1.8	1.0
1	2	3																	
7.5	5.0	5.0																	
5.5	3.5	3.5																	
2.0	1.8	1.0																	
K4 1.5	2.0			1 pitted - pitting denser - abundant micropits	2 destroyed pitting - cannot distinguish individual pits - little lichen	3 large pits - some irregular in shape													
K5 10.0	2.0	5.2		1 clint surface - simpler than previous areas - all pits destroyed - thick flaking	2 vegetated grike - soil and vegetation in grikes	3 pan - small shallow pan K1- plate A VII-4 K2- A VII-5 K3- A VII-6 K4- A VII-7 K5- A VII-8 in appendix VI													

TABLE AVI.1

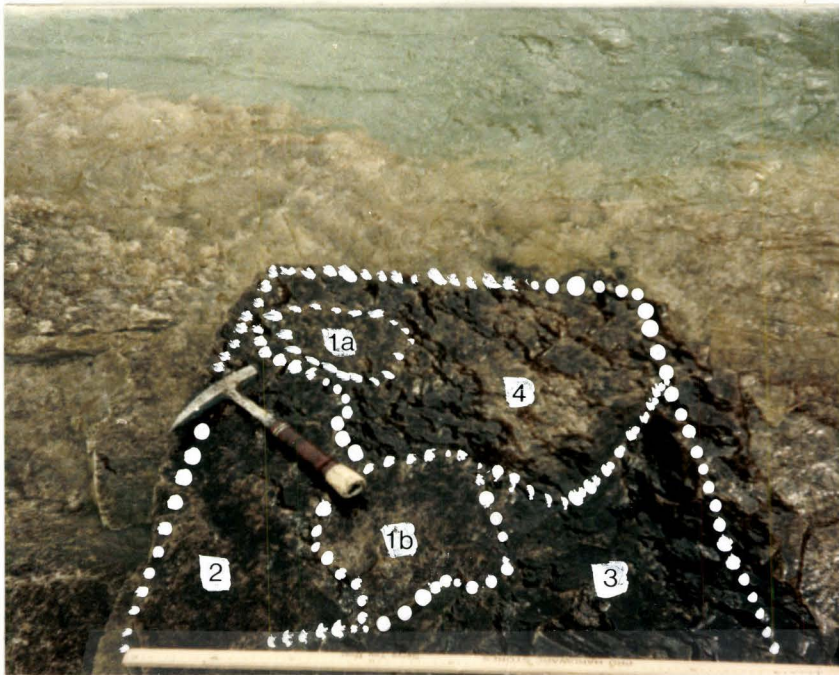


Plate AVI.4

- detailed karren site K1, Cyprus Lake
- 0 m away from water
- 0 m above water
- reference pages 27-31

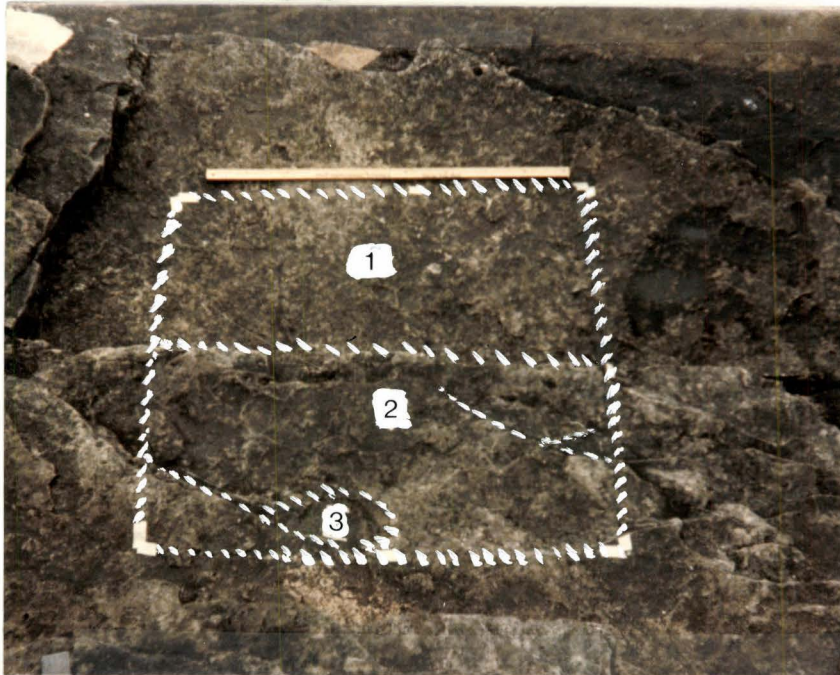


Plate AVI.5

- detailed karren site K2, Cyprus Lake
- 0.5 m away from water
- 0.5 m above water
- reference pages 27-31



PLate AVI.6

-detailed karren site K3-1, K3-2, K3-3

K3-1 - intermediate exposure age

K3-2 - old exposure age

K3-3 - young exposure age

-1.75 m away, 1.5 m above water

-reference pages 27-31

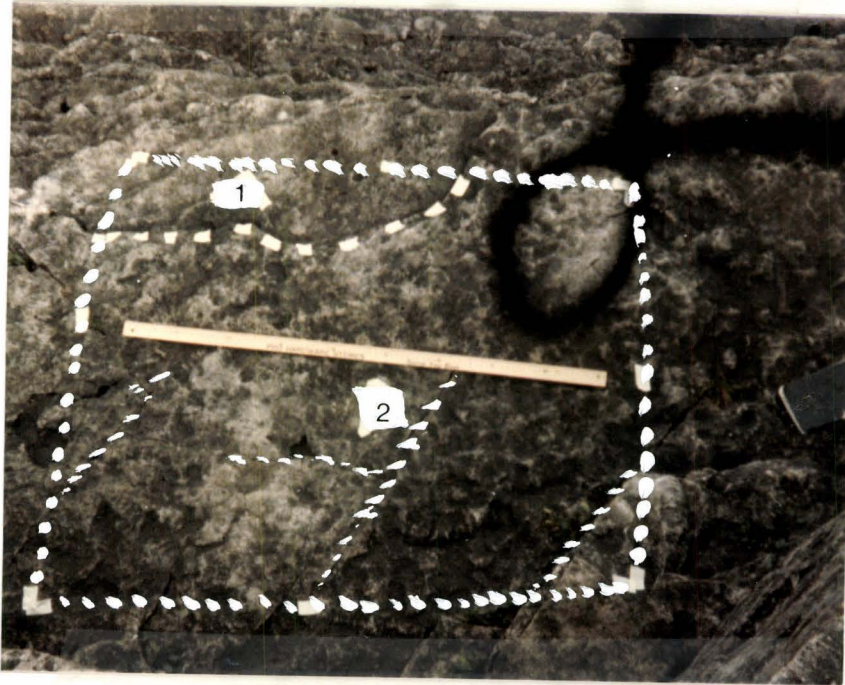


Plate AVI.7

- detailed karren site K4, Cyprus Lake
- 1.5 m away, 2.0 m above water
- reference pages 27-31



Plate AVI.8

- detailed karren site K5, Cyprus Lake
- 10.0 m away, 2.0 m above water
- reference pages 27-31

APPENDIX-VII INLAND PAVEMENT

The Dyers Bay sample site was a small, well developed, roadside section of Amabel kluft karren pavement (plate AVII.1) located approximately 3/4 of a mile inland it is doubtful that the area was submerged even during the high Nippising Lake level stage. Many troughs (rundkarren) drain into three main fissures. Both the grikes and rundkarren had well rounded lips indicative of soil covered solution. Dirt, vegetation and pebbles filled the grikes to varying extents. Partially intact centre pieces existed in 2 locations of grike "G3" (Plate AVII.2).

The clints revealed single pits often found in the bottom of rounded rundkarren channels (Plate AVII.3).

Grike dimensions were taken at 1 meter intervals revealing average widths of 15.9, 7.7, and 10.8 cm and average depth of 26.0, 30.6, and 42.6 cm for G1, G2 and G3 respectively.

Samples taken from G1 grike and the clint surface were white interlocking micro crystalline dolomite with insoluble percentages of 4.5% and 6.4% respectively.

It was not possible to measure accurate shoreline to grike distances as at Cyprus Lake and Bear's Rump Island. Consequently statistical analysis of Dyer's bay grike and rundkarren dimensions was not conducted. General observational differences exist between such inland pavements and coastal pavements. Greater excavation of grikes is apparent. The rounded nature of the pavement suggest biogenic acidic effects in the solution process. Pits are less abundant, possibly formed by a different mechanism

than the spray wash littoral pits at Bear's Rump and Cyprus Lake. Fig 5.0.1 is the plan view of Dyer's bay sample site. Immediate emphasis must be placed on the secondary solution "rundkarren" channels which drain into the grikes. These were not seen at any of the coastal locations, indicating that vegetation intensified solution has been active for longer periods inland resulting in well developed secondary karren features.

The striking difference between inland and coastal pavement is due to burial of the bedrock, biologically increased solution, and subsequent exposure

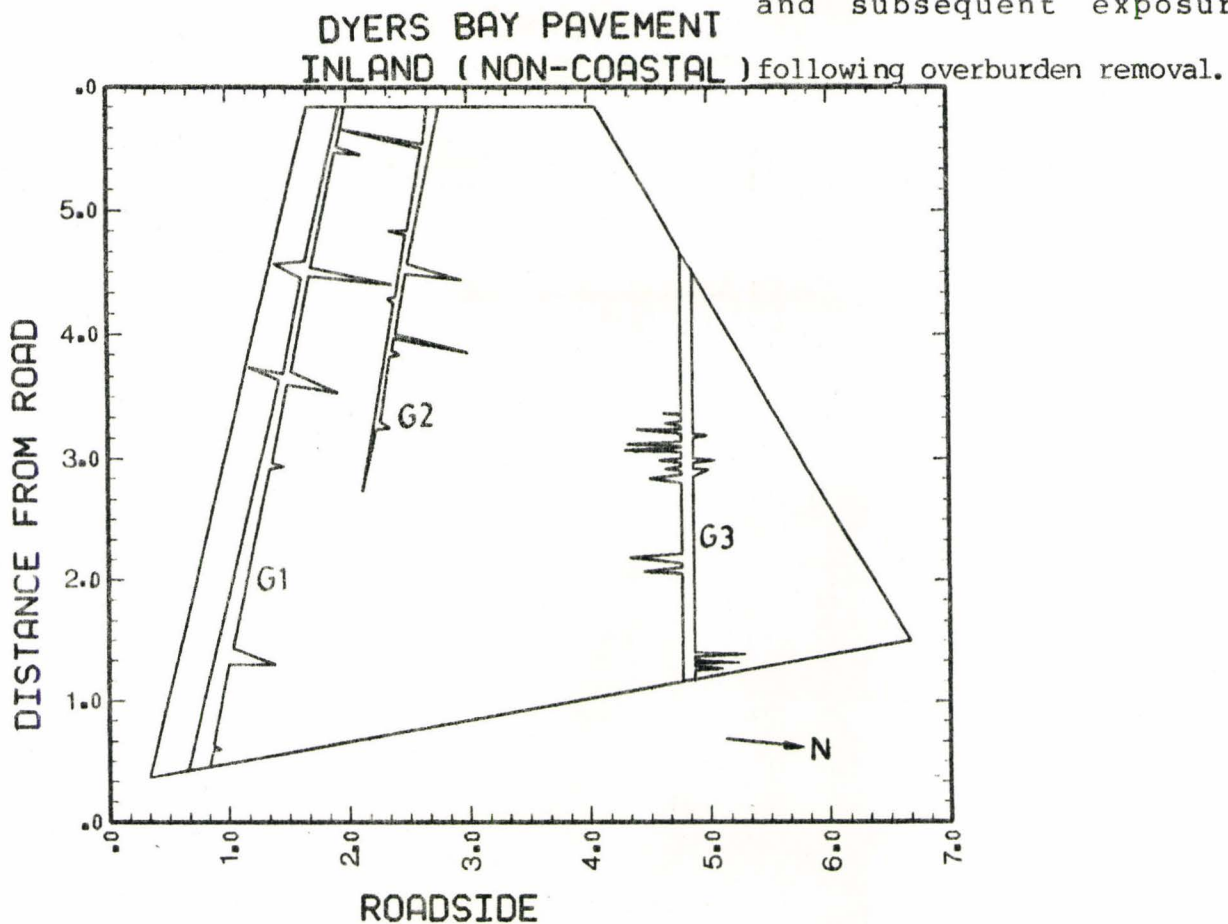




Plate AVII.1



Plate VII,2



Plate VII3

LIST OF ABBREVIATIONS

Abbreviation

BRI Bear's Rump Island
MBS Master Bedding Surface
SS Sample Strip

LIST OF REFERENCES

- Bell, B. 1985. "Pit Karren Formation on The Northern Bruce Peninsula"
An undergraduate thesis
- Blatt, H., Middleton, J., Murray. 1980.
"Origin Of Sedimentary Rocks"-edition 2
Prentice-Hall, Inc., Englewood Cliffs,
New Jersey
- Cowell, D. W. 1976. "Karst Geomorphology of the Bruce Peninsula"
Masters of Science thesis
- Cvijic, J. 1960. "La Geographie Des Terrains Calcaires-Beograd" Navemo Delo 212 p
- Drake, J.J., Ford, D.C., Gascone, M. 1982.
"Notes on the Solution of Karst Rocks"
Department of Geography, McMaster Univ.
- Drew, D. P. 1983. "Accelerated Soil Erosion in a Karst Area: The Burren, Western Ireland"
Journal of Hydrology ISSN 0022-1694
vol 61 p45
- Ford, D.C. 1984 Ch 4 of "Final Report, Resource Management Study of Caves-, Tobermory Is. Unit, Georgian Bay Is. National Park"
Parks Canada 1984
- Ford, D. C. 1983. "Effects of Glaciations Upon Karst Aquifers in Canada"
Journal of Hydrology 0022-1694, v 61 p149
- Ford, D. C. "A Review of Alpine Karst in the Southern Rocky Mountains of Canada"
- Ford, D. C. "Threshold and Limit Effects on Karst Geomorphology"
- Goodchild, M. F. 1984. "Final Report, Resource Management Study of Caves-, Tobermory Is. Unit, Georgian Bay Is. National Park"
Department of Geography, University of Western Ontario, Parks Canada 1984
- Grosset, C. 1985. "Cobble Beaches"
Undergraduate Thesis

- Jennings 1971. "Karst", Mass. : MIT Press, 225p
- Norcliff, G. B. 1977. "Inferential Statistics for Geographers"
Hutchinson & Co. Ltd.
- Pluhar, A. 1966. "Lapies and Related Small Karst Features on the Niagara Escarpment"
A MA thesis, McMaster University
- Ritter, D. F. 1978. "Process Geomorphology"
Dubque Iowa: W.C. Brown Co.
- Sweeting, M. M. 1973. "Karst Landforms"
New York Columbia University Press
- Williams, G. P. 1979. "Adjustment of the Fluvial system:"
a proceedings vol. of 10th Ann. Geomorph.
Symposia Series at Brighampton, New York
Kendall/hont Pub. Co.